Supporting Information

Synthesis and characterization of 5-(2-fluoro-4-[^{11}C]methoxyphenyl)-2,2-dimethyl-3,4-dihydro-2*H*-pyrano[2,3-*b*]pyridine-7-carboxamide as a PET imaging ligand for metabotropic glutamate receptor 2

Gengyang Yuan,[†,*] Maeva Dhaynaut,[†] Yu Lan,[‡] Nicolas J. Guehl,[†] Dalena Huynh,[†] Suhasini M. Iyengar,[‖] Sepideh Afshar,[†] Manish Kumar Jain,[&] Julie E. Pickett, [&] Hye Jin Kang,[&] Hao Wang,[‡] Sung-Hyun Moon,[†] Mary Jo Ondrechen,[‖] Changning Wang,[‡] Timothy M. Shoup, [†] Georges El Fakhri,[†] Marc D. Normandin,[†] Anna-Liisa Brownell[†,*]

[†]Gordon Center for Medical Imaging, Massachusetts General Hospital and Harvard Medical School, 3rd Avenue, Charlestown, MA 02129, USA

[‡]Athinoula A. Martinos Center for Biomedical Imaging, Massachusetts General Hospital and Harvard Medical School, Charlestown, Massachusetts 02129, USA

[‖]Department of Chemistry and Chemical Biology, Northeastern University, 360 Huntington Avenue, Boston, MA 02115, USA

[&] Department of Pharmacology, University of North Carolina at Chapel Hill School of Medicine, Chapel Hill, NC 27599, USA

Corresponding Authors

[*]G.Y.: phone 857-210-6386; email, gyyuan@mgh.harvard.edu; ORCID ID: https://orcid.org/0000-0003-4817-0052

[*]A-L.B.: phone 617-744-3725; email, abrownell@mgh.harvard.edu; ORCID ID: https://orcid.org/0000-0002-3814-868X

Table of Contents

Supporting Information:

1. *In vitro* functional assays of compounds 12 and 13 against mGluR2

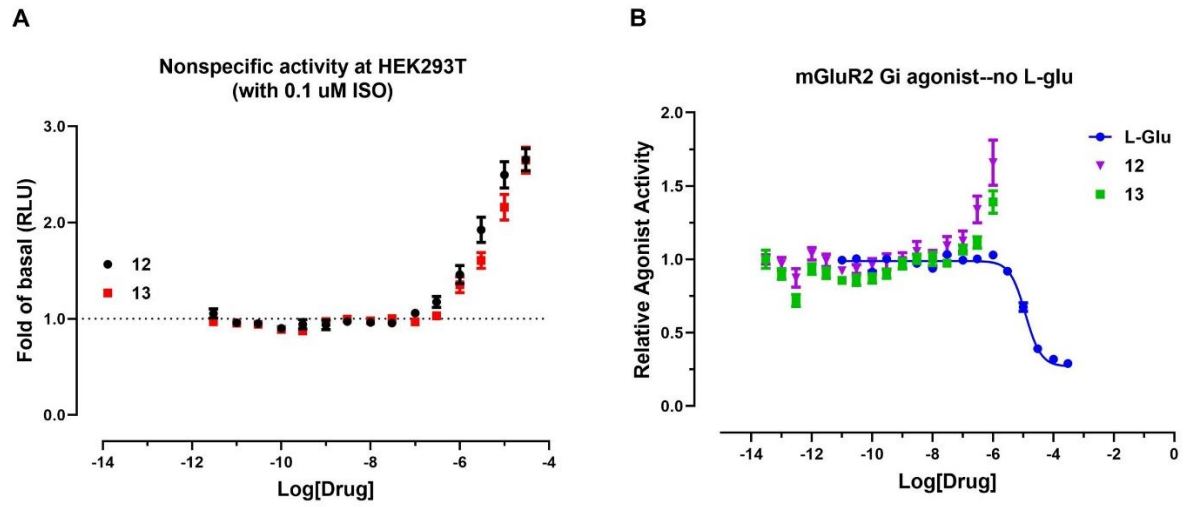

Figure S1. *In vitro* characterization of compounds **12** and **13** in the GloSensor assay. (**A**) Both **12** and **13** showed nonspecific activity in untransfected HEK293T cells at or above 300 nM in the presence of 0.1 μM isoproterenol (ISO); (**B**) mGluR2 stably expressing cells in a tetracycline-inducible manner were induced with 1 μg/mL tetracycline, and no agonist activity was observed for compounds **12** and **13**.

2. Preparation of mGluR2 homology model for NAMs:

The homology model is available for download at:

https://drive.google.com/file/d/1MPt5Wo6kYxxxcrySDYMPMyR9EJUVCAc2/view?usp=sharing

The target sequence of 872 residues used for building the model structure for mGluR2 is listed below:

MGSLLALLALLLLWGAVAEGPAKKVLTLEGDLVLGGLFPVHQKGGPAEDCGPVNEHRGIQ
RLEAMLFALDRINRDPHLLPGVRLGAHILDSCSKDTHALEQALDFVRASLSRGADGSRHI
CPDGSYATHGDAPTAITGVIGGSYSDVSIQVANLLRLFQIPQISYASTSAKLSDKSRYDY
FARTVPPDFFQAKAMAEILRFFNWTYVSTVASEGDYGETGIEAFELEARARNICVATSEK
VGRAMSRAAFEGVVRALLQKPSARVAVLFTRSEDARELLAASQRLNASFTWVASDGWGAL
ESVVAGSEGAAEGAITIELASYPISDFASYFQSLDPWNNSRNPWFREFWEQRFRCSFRQR
DCAAHSLRAVPFEQESKIMFVVNAVYAMAHALHNMHRALCPNTTRLCDAMRPVNGRRLYK
DFVLNVKFDAPFRPADTHNEVRFDRFGDGIGRYNIFTYLRAGSGRYRYQKVGYWAEGLTL
DTSLIPWASPSAGPLPASRCSEPCLQNEVKSVQPGEVCCWLCIPCQPYEYRLDEFTCADC
GLGYWPNASLTGCFELPQEYIRWGDAWAVGPVTIACLGALATLFVLGVFVRHNATPVVKA
SGRELCYILLGGVFLCYCMTFIFIAKPSTAVCTLRRLGLGTAFSVCYSALLTKTNRIARI
FGGAREGAQRPRFISPASQVAICLALISGQLLIVVAWLVVEAPGTGKETAPERREVVTLR
CNHRDASMLGSLAYNVLLIALCTLYAFKTRKCPENFNEAKFIGFTMYTTCIIWLAFLPIF
YVTSSDYRVQTTTMCVSVSLSGSVVLGCLFAPKLHIILFQPQKNVVSHRAPTSRFGSAAA
RASSSLGQGSGSQFVPTVCNGREVVDSTTSSL

A hybrid model was generated in YASARA[1] from the above sequence and the template structures with the PDB IDs, 4OO9,[2] 4OR2,[3] 6N52[4] and 5KZN[5]. These structures were obtained from a BLAST search against the PDB of the above mGluR2 sequence.[6] YASARA generated 17

models initially from these structures and finally a hybrid model was generated using the best parts from these 17 initial models, to achieve a higher quality score and a more accurate final model. Figure S2 shows the hybrid model generated in YASARA with initial model in blue and hybridized parts in different colors. The resulting hybrid model obtained the following quality Z-scores (Table S1).

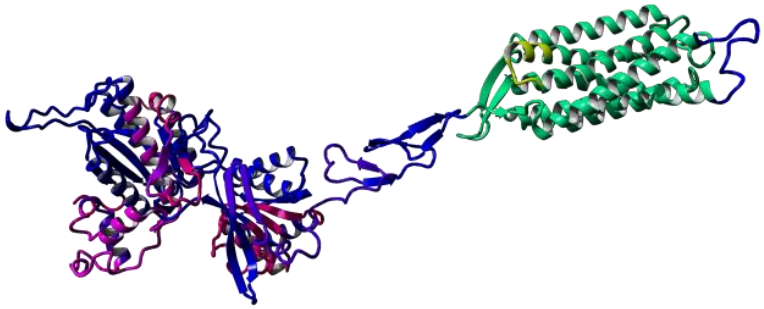

Figure S2: The figure shows the initial model in blue, and all hybridized parts in different colors

Table S1: Z-Scores for the hybrid model generated on YASARA

Check type	Quality Z-score	Comment
Dihedrals	0.043	Good
Packing 1D	-0.082	Good
Packing 3D	-1.216	Satisfactory
Overall	-0.591	Good

3. Structural evaluation of mGluR2 model

This hybrid model was further validated by the following methods.

3.1 MODFOLD results

The hybrid model was validated using ModFOLD.[7] The confidence for this model is rated as HIGH with a p-value of 1.001 E-3 and with the global model quality score of 0.4433, indicating

that it is a complete and confident model for mGluR2. The p-value represents the probability of the model being incorrect. With a p-value for this model of 0.001001, there is only a 1/1001 chance that this model is incorrect.

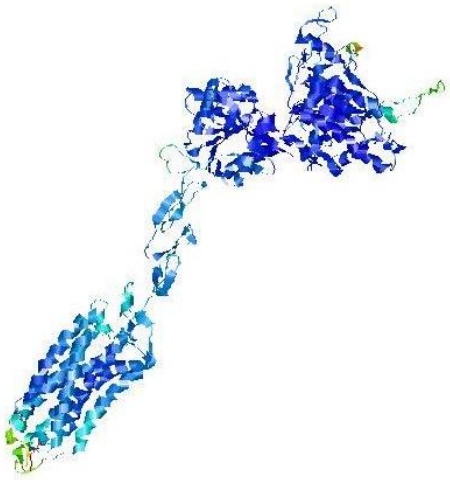

Figure S3: This image was generated by ModFOLD based on residue accuracy prediction for the model. Blue is for highest accuracy, with the green, yellow, orange, and red indicating successively lower accuracy.

3.2 Structure Analysis Verification Server (SAVES) results

The second server used to validate this model was SAVES[8-10] and its components, VERIFY 3D and ERRAT. VERIFY 3D scores are reported as a function of sequence number for the model. As Figure S3 shows, VERIFY 3D assigned a 3D-1D score of > 0.2 for at least 87.23% of the amino acids. This implies that the model is compatible with its sequence.

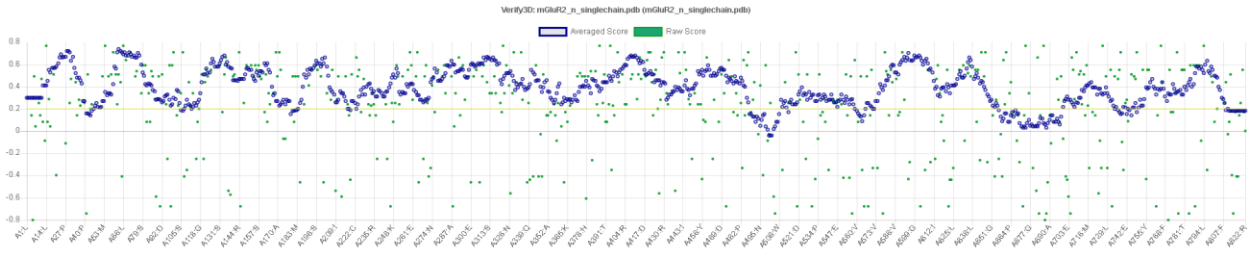

Figure S4: Verify 3D scores for the hybrid model

ERRAT scores likewise are reported as a function of sequence number for the hybrid model generated by YASARA. As shown in Figure S5, green indicates a good score, yellow represents regions that can be rejected at 95% confidence and red symbolizes regions that can be rejected at 99% confidence. As Figure S5 shows, the hybrid model contains significantly low red colored regions. The quality factor for this model is 95.9. Therefore, it is a good model according to ERRAT.

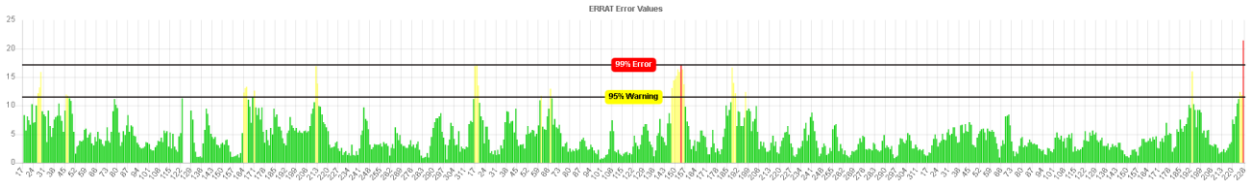

Figure S5: ERRAT scores for the hybrid model

3.3 SWISS Model-QMEAN results

QMEAN is a composite scoring function which derives both global and local absolute quality estimates based on one single model.[9] The QMEAN score for this hybrid model is -1.43. Below is an image showing the sequence of the protein colored by local quality.

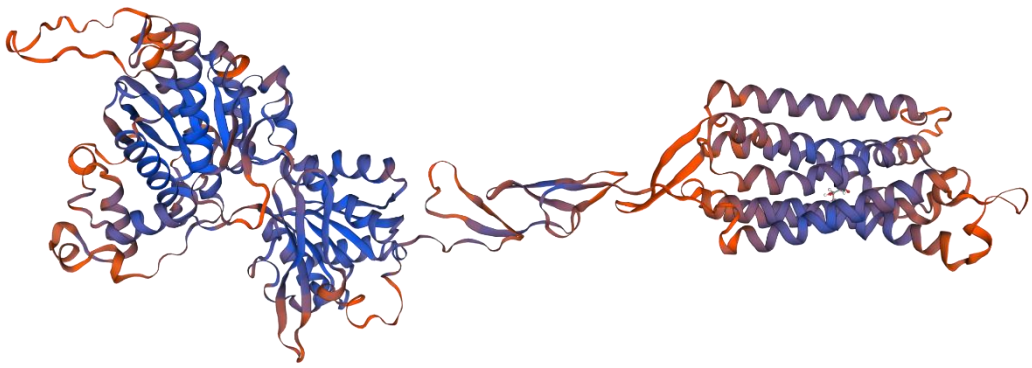

Figure S6: Image generated by QMEAN showing the local quality of the hybrid model. Blue indicates better quality regions; orange indicates lower quality regions.

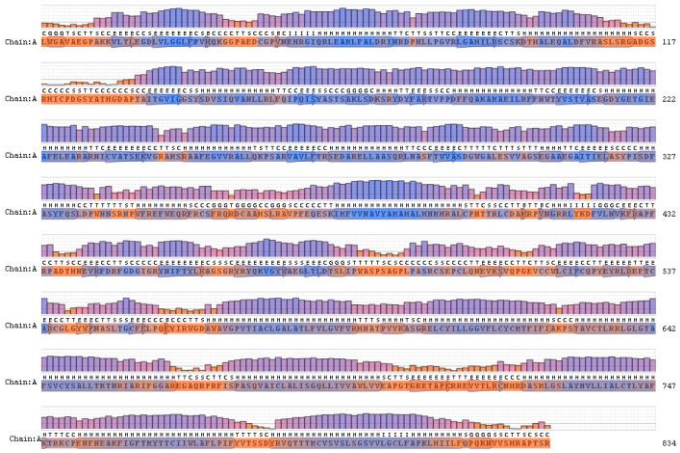

Figure S7: Image showing the local quality of the structure as a function of sequence number, generated by QMEAN.

3.4 Ramachandran Plot:

The hybrid model generated by YASARA was further evaluated via Ramachandran plot. As Figure S8 shows 89.6% (643) of the residues lie in the favored regions and 10.2% (73) lie in the additionally allowed regions. Only 0.1% of all residues, corresponding to only one residue, in the generously allowed regions and no residues in disallowed regions. This is further evidence of a quality model structure.

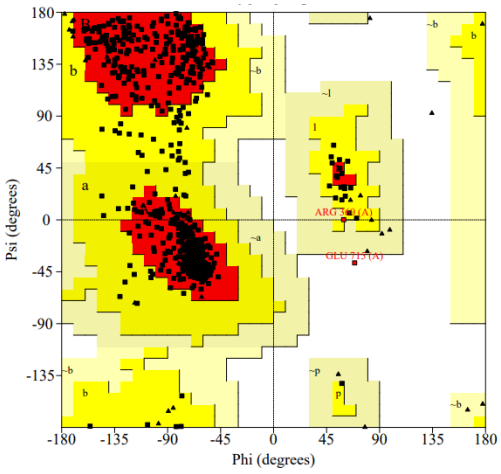

Figure S8: A Ramachandran plot for the hybrid model. Plot generated with the SAVES server.

4. Prediction of Binding Site

Partial Order Optimum Likelihood (POOL)[11-12] was used to predict the key binding residues in the allosteric binding site. POOL is based on computed electrostatic and chemical properties calculated from the three-dimensional structure of the query protein[13] and has been shown to be effective for homology model structures.[14] The identified top residues are listed below and the ones that are reported previously are highlighted in bold.[15-16]

Cys560, Cys606, Leu609, Cys616, Tyr617, **Phe623**, **Arg635**, Arg636, Gly638, Leu639, Gly640, Thr641, **Phe643**, Val645, Cys646, Tyr647, Leu650, Lys653, Cys683, **His723**, Tyr734, **Asn735**, Ile739, Cys742, Tyr781, Tyr787, Cys795, Val798, Ser801, Lys813.

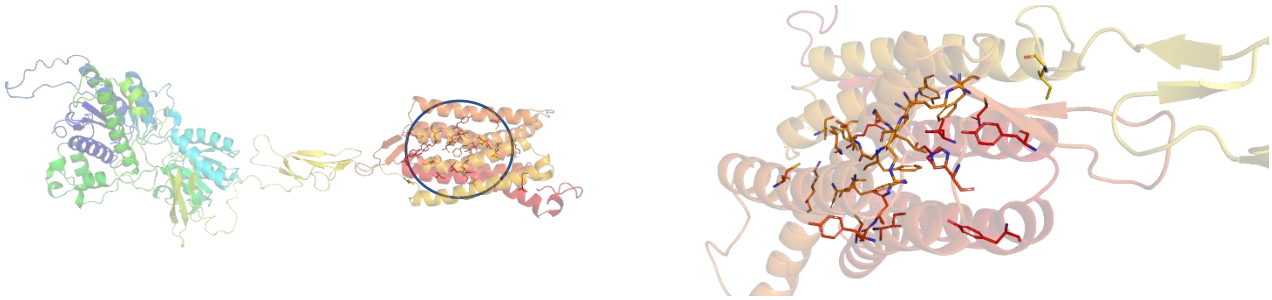

Figure S9: Position of the allosteric binding site for NAMs.

5. Purification and confirmation of [^{11}C]13

Figure S10 shows the semi-preparative HPLC spectra for the purification of [^{11}C]**13** from the reaction mixture. The HPLC radioactivity trace is shown at the top and the UV trace is shown at the bottom. The retention time of [^{11}C]**13** was 8.62 min under the following HPLC conditions: Column: Waters XBridge, C18, 250 × 10 mm, 5 μ; Wavelength of 254 nM; Mobile phase: acetonitrile/water/Et_3N (50/50/0.1%) at a flow rate of 5 mL/min.

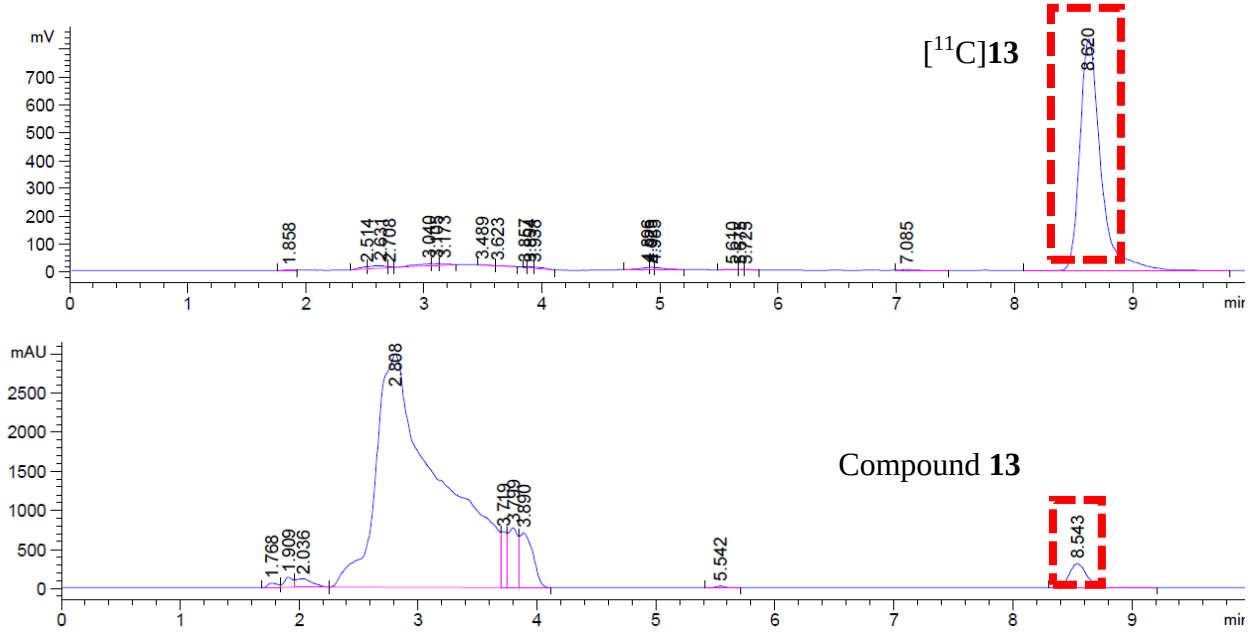

Figure S10. Purification of [^{11}C]**13** from reaction mixture via semi-preparative HPLC. The HPLC radioactivity trace is shown at the top and the UV trace is shown at the bottom.

The identity of the purified and formulated [^{11}C]**13** was confirmed by co-injecting with the unlabeled compound **13** in an analytical HPLC system (Figure S11). The radioHPLC trace of [^{11}C]**13** spectrum is shown in black (top) and the UV Trace of reference **13** is shown in blue (bottom). The retention time of [^{11}C]**13** was 8.11 min under the following HPLC conditions: Column: Waters, XBridge, C18, 4.6 × 150 mm 3.5 μ; Wavelength of 254 nM; Mobile phase: acetonitrile/water/Et_3N (45/55/0.1%) at a flow rate of 1 mL/min.

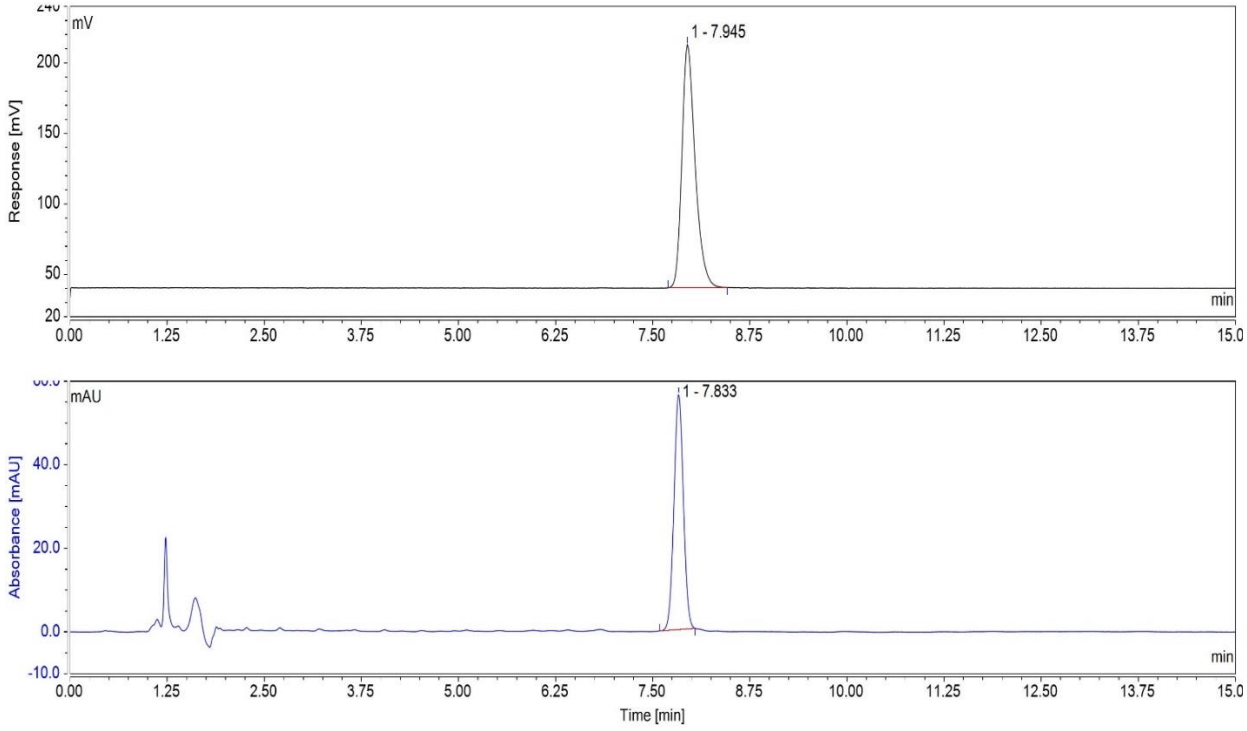

Figure S11. Analytical HPLC Spectra for formulated [^{11}C]**13**. The radioHPLC trace of [^{11}C]**13** spectrum is shown in black (top) and the UV Trace of reference **13** is shown in blue (bottom).

6. Prediction of the metabolism sites of 13 with SMARTCyp[17]

Table S2. Prediction of the metabolism sites of **13** with SMARTCyp

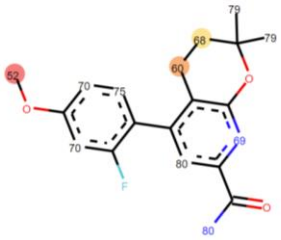

3A4 Ranking	Atom	3A4 Score	Energy	2DSASA	Span2end	Relative Span	Similarity
1	C.22	51.5	62.2	66.4	0	1.0	1.0
2	C.18	59.6	66.4	25.1	3	0.7	0.3
3	C.17	68.2	75.9	28.4	2	0.8	0.3
4	N.6	68.6	75.6	10.9	2	0.8	0.3
5	C.9	70.3	77.2	27.8	3	0.7	0.7
6	C.11	70.3	77.2	26.2	3	0.7	0.3
7	C.8	74.8	80.8	23.3	4	0.6	0.7
8	C.19	79.3	89.6	58.5	0	1.0	0.3
9	N.24	80.3	89.6	50.6	1	0.9	0.7
10	C.2	80.5	86.3	17.3	4	0.6	0.3

7. HPLC spectra for compounds 12-13

The purity of compounds **12-13** was determined by the Agilent 1200 series HPLC system, which is part of the LC-MS system, equipped with an Agilent Eclipse C8 analytical column (150 mm × 4.6 mm, 5 μm). Elution was with a 0.1% formic acid solution of water (A) and acetonitrile (B). The wavelength of UV detector was 254 nm.

A gradient elution method was used for compounds **12** and **13**: 0 min, 95% A, 5% B (5% acetonitrile); 0-3.0 min (5% acetonitrile to 95% acetonitrile) linear increase; 3.0-4.5 min (95% acetonitrile) isocratic; 4.5-5.0 min (95% acetonitrile to 5% acetonitrile) linear decrease; 5.0-7.0 min (5% acetonitrile) isocratic. The flow rate was 0.7 mL/min. Purities of all new compounds were determined using the area percentage method on the UV trace scanning under a wavelength of 254 nm. All compounds are >95% pure by HPLC analysis.

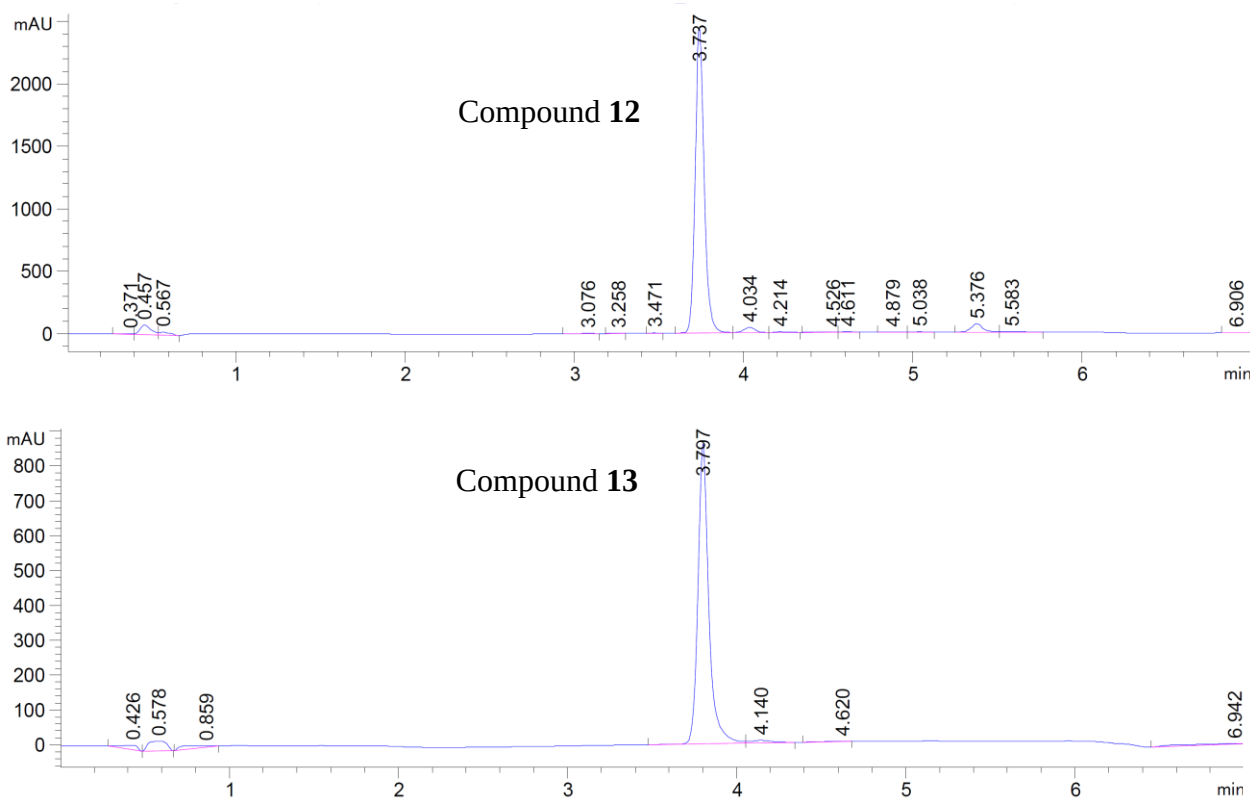

Figure S12. HPLC spectra for compounds **12** (top) and **13** (bottom).

8. NMR spectra

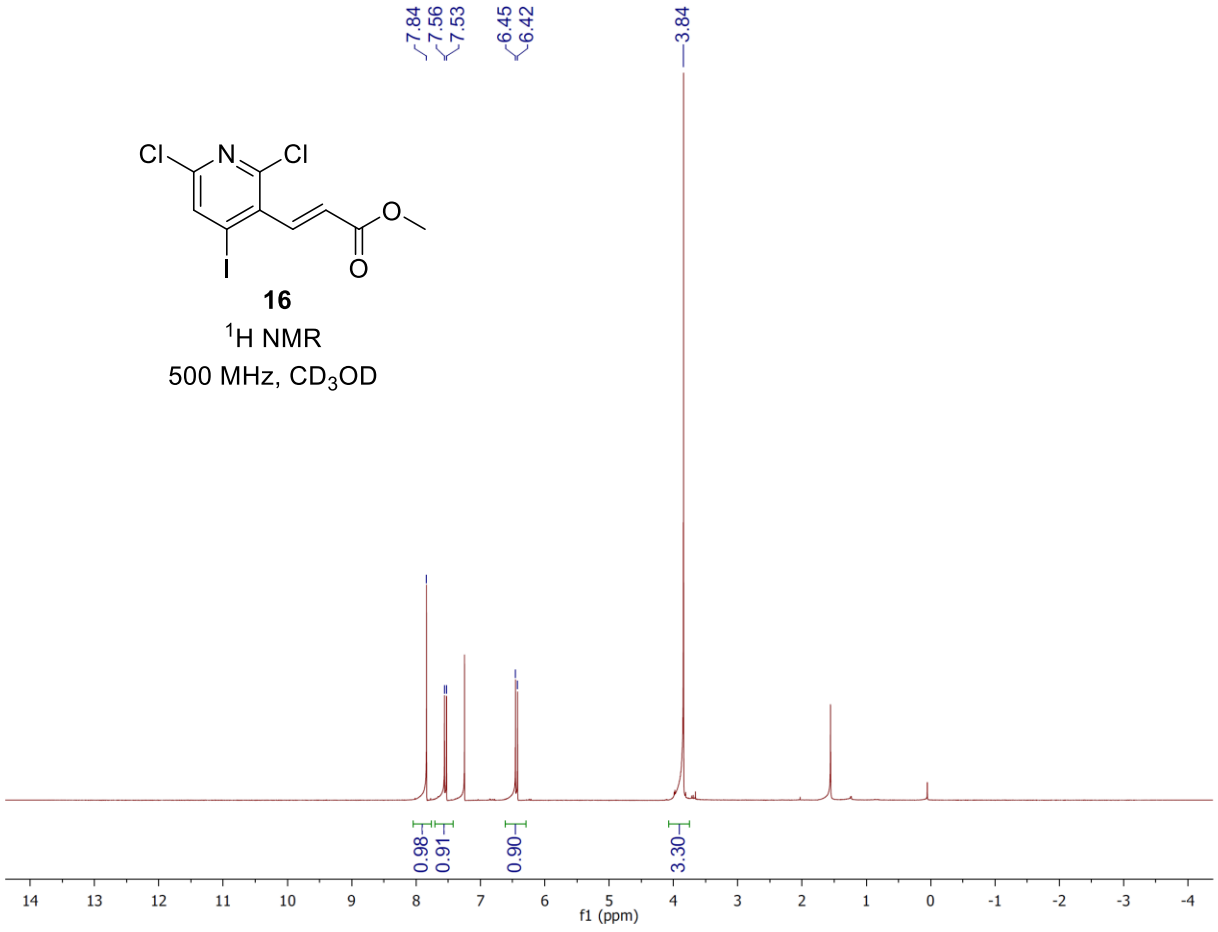

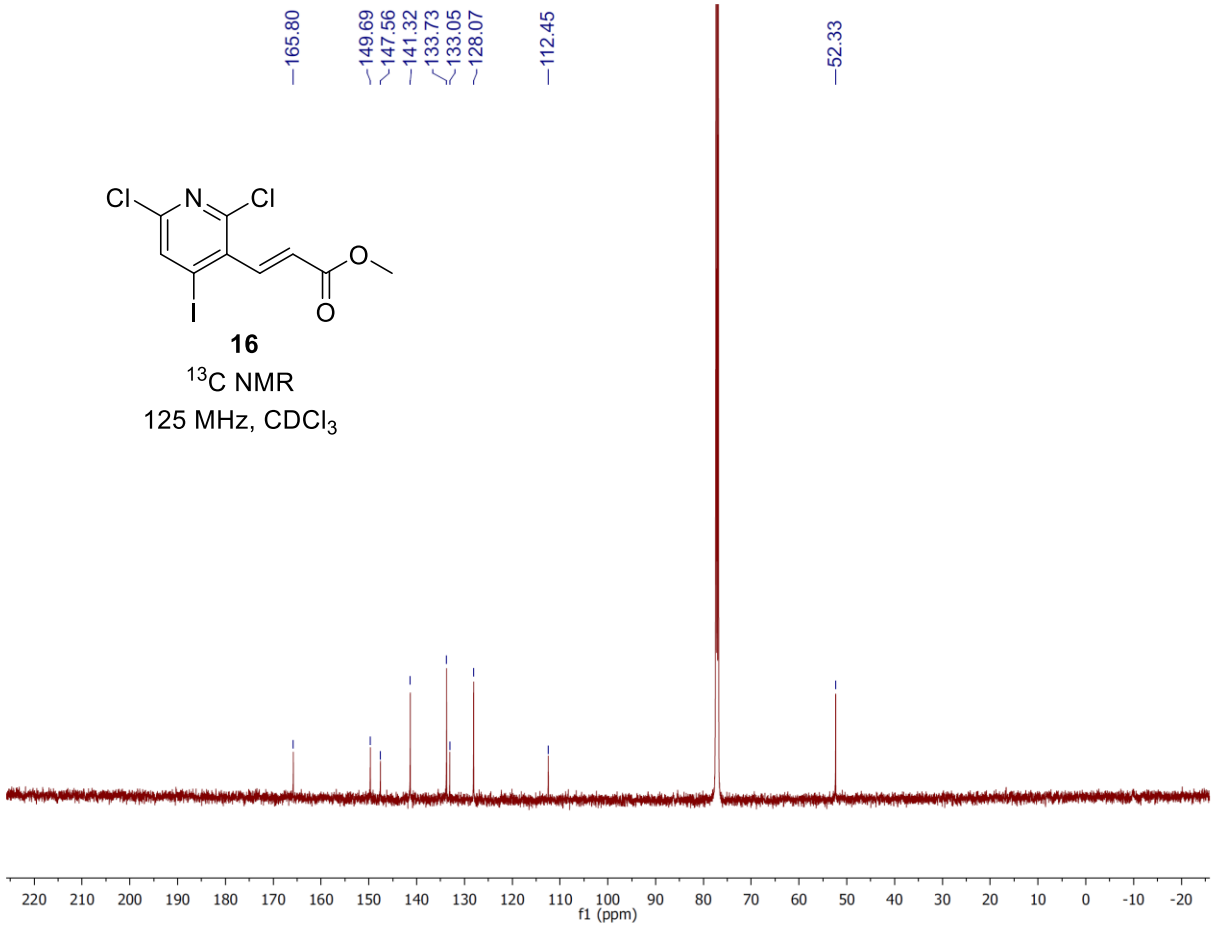
165.80
149.69
147.56
141.32
133.73
133.05
128.07
112.45
52.33
Cl
N
Cl
O
O
I
16
13C NMR
125 MHz, CDCl3
220 210 200 190 180 170 160 150 140 130 120 110 100 90 80 70 60 50 40 30 20 10 0 -10 -20
f1 (ppm)

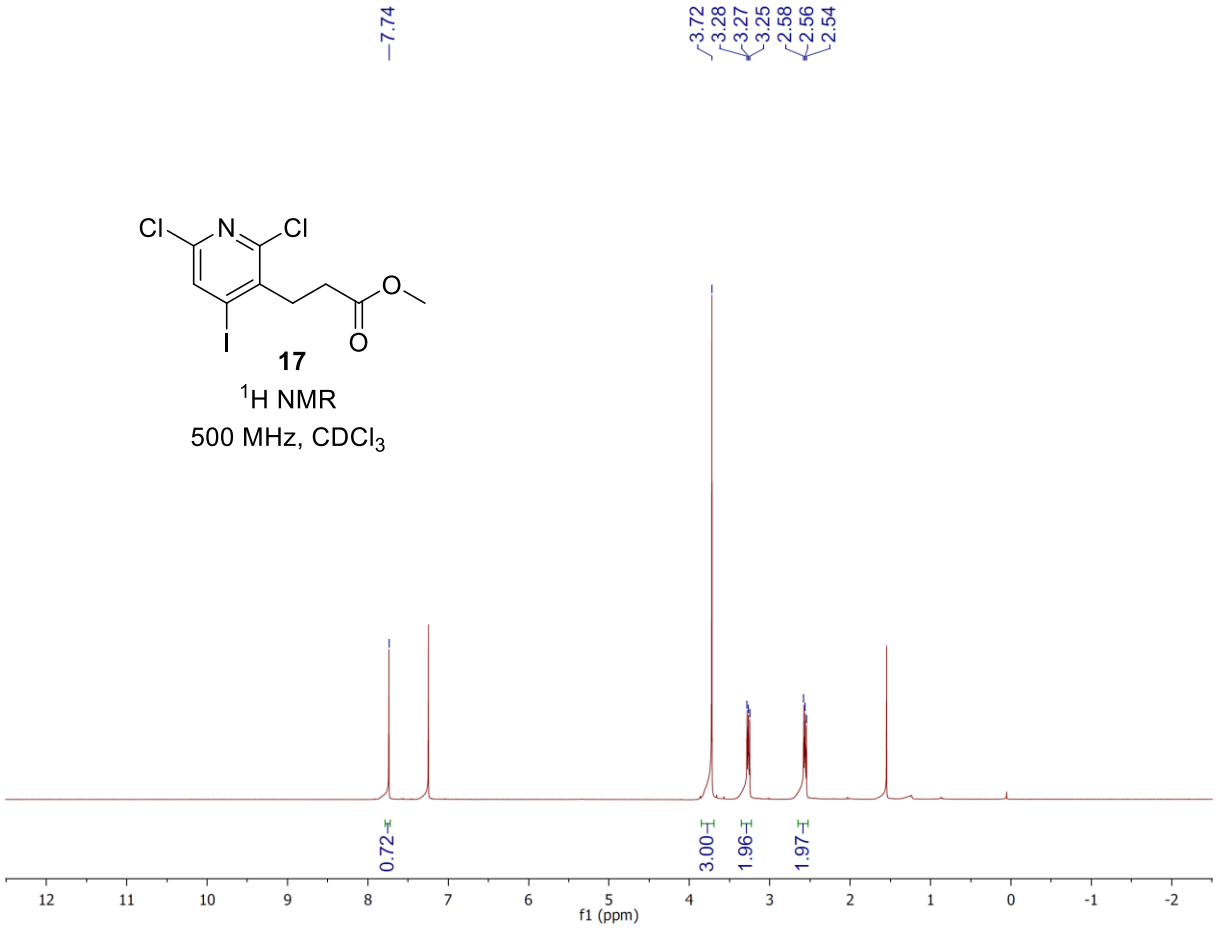

17

^{1}H NMR

500 MHz, $CDCl_3$

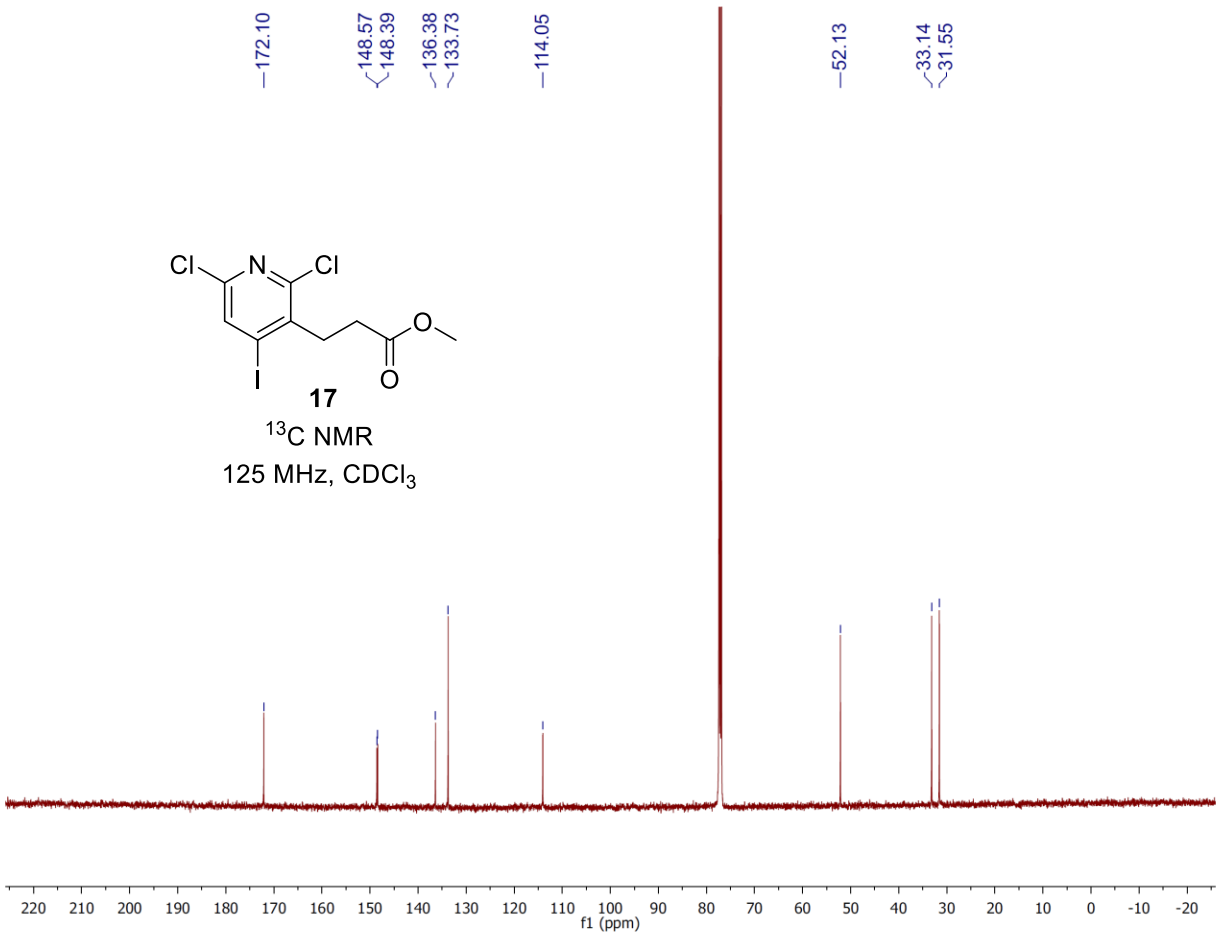
172.10
148.57
148.39
136.38
133.73
114.05
52.13
33.14
31.55
Cl
N
Cl
O
I
O
17
13C NMR
125 MHz, CDCl3
220 210 200 190 180 170 160 150 140 130 120 110 100 90 80 70 60 50 40 30 20 10 0 -10 -20
f1 (ppm)

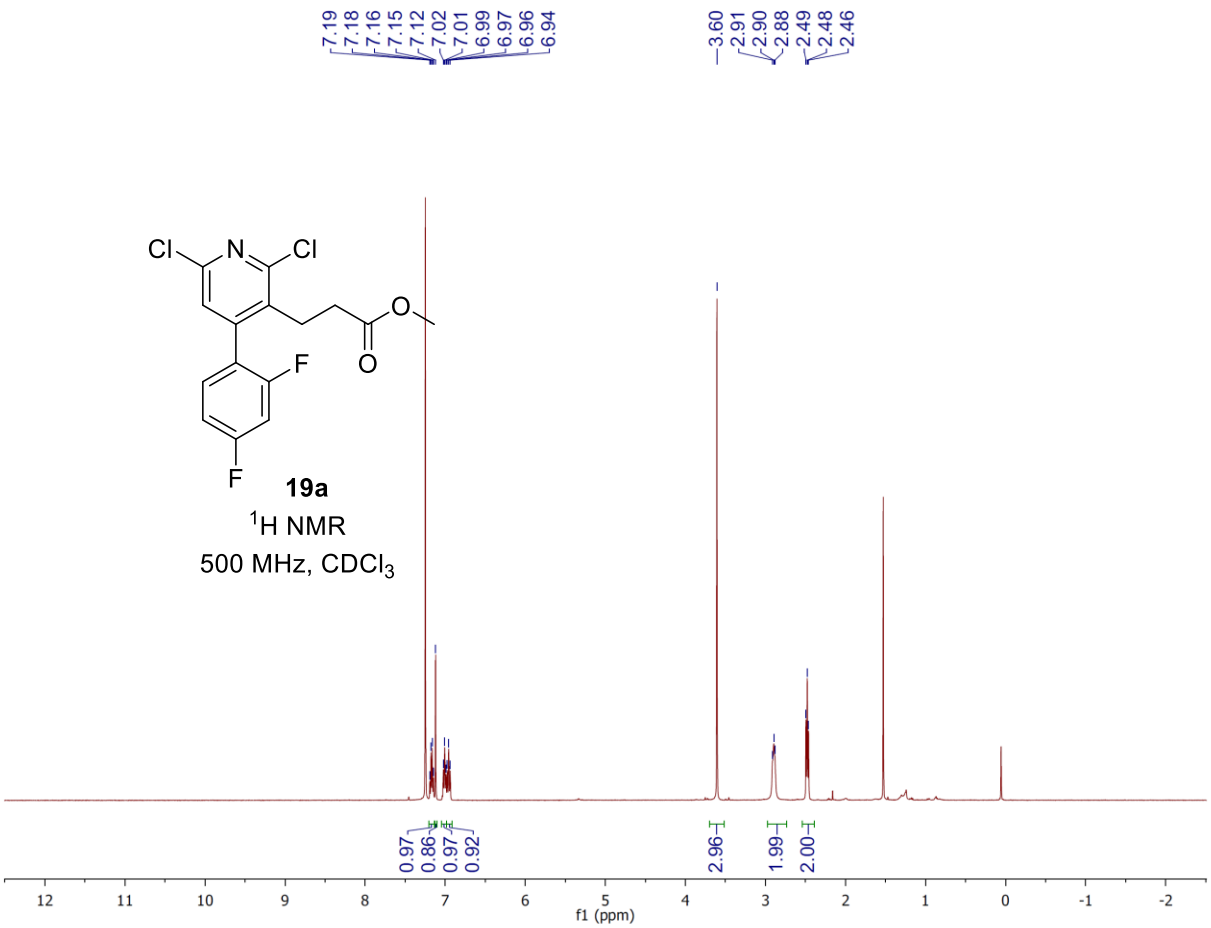
7.19
7.18
7.16
7.15
7.12
7.02
7.01
6.99
6.97
6.96
6.94
3.60
2.91
2.90
2.88
2.49
2.48
2.46
Cl
N
Cl
O
F
O
F
19a
1H NMR
500 MHz, CDCl3
0.97
0.86
0.97
0.92
2.96
1.99
2.00
12
11
10
9
8
7
6
5
4
3
2
1
0
-1
-2
f1 (ppm)

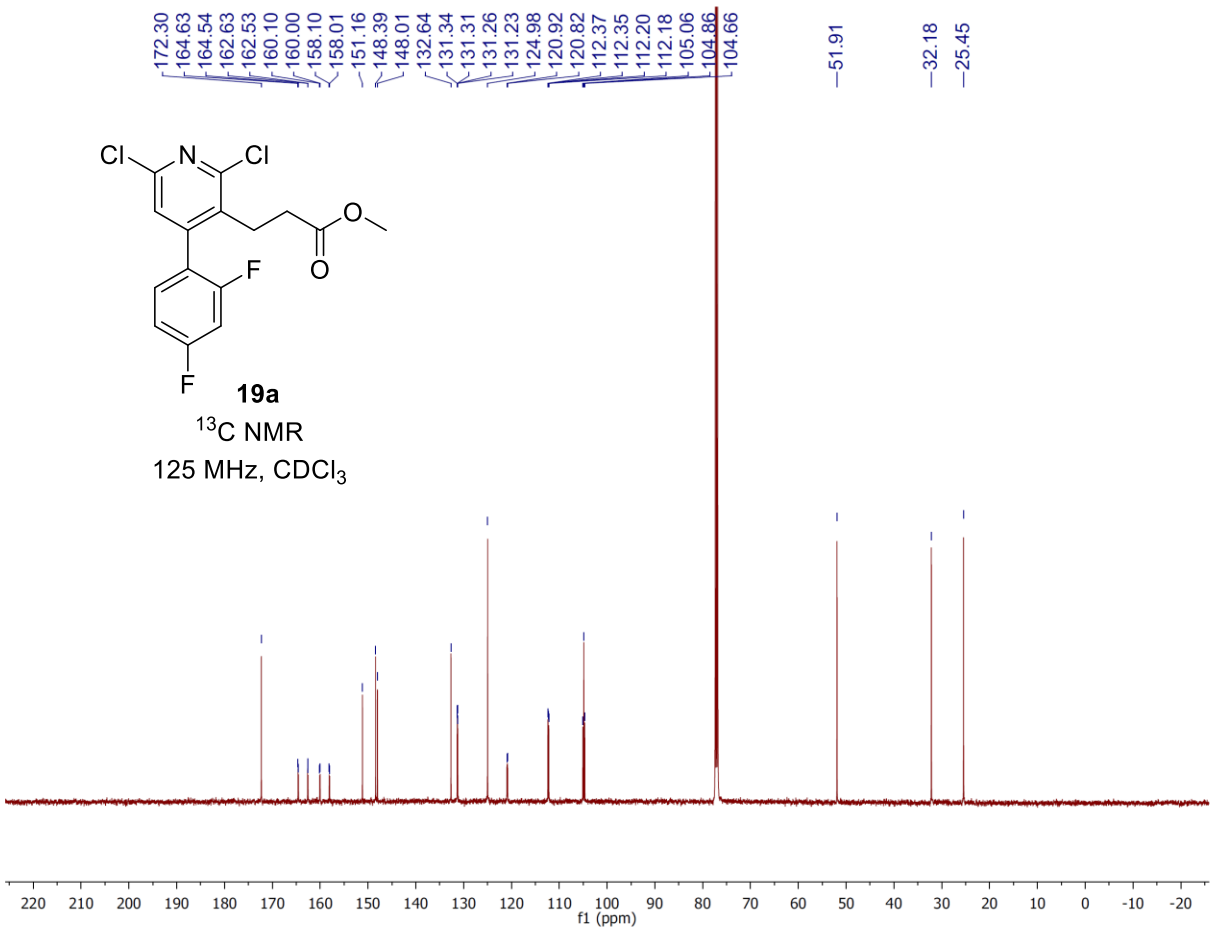
172.30
164.63
164.54
162.63
162.53
160.10
160.00
158.10
158.01
151.16
148.39
148.01
132.64
131.34
131.31
131.26
131.23
124.98
120.92
120.82
112.37
112.35
112.20
112.18
105.06
104.86
104.66
51.91
32.18
25.45
Cl
N
Cl
O
O
F
F
19a
13C NMR
125 MHz, CDCl3
220 210 200 190 180 170 160 150 140 130 120 110 100 90 80 70 60 50 40 30 20 10 0 -10 -20
f1 (ppm)

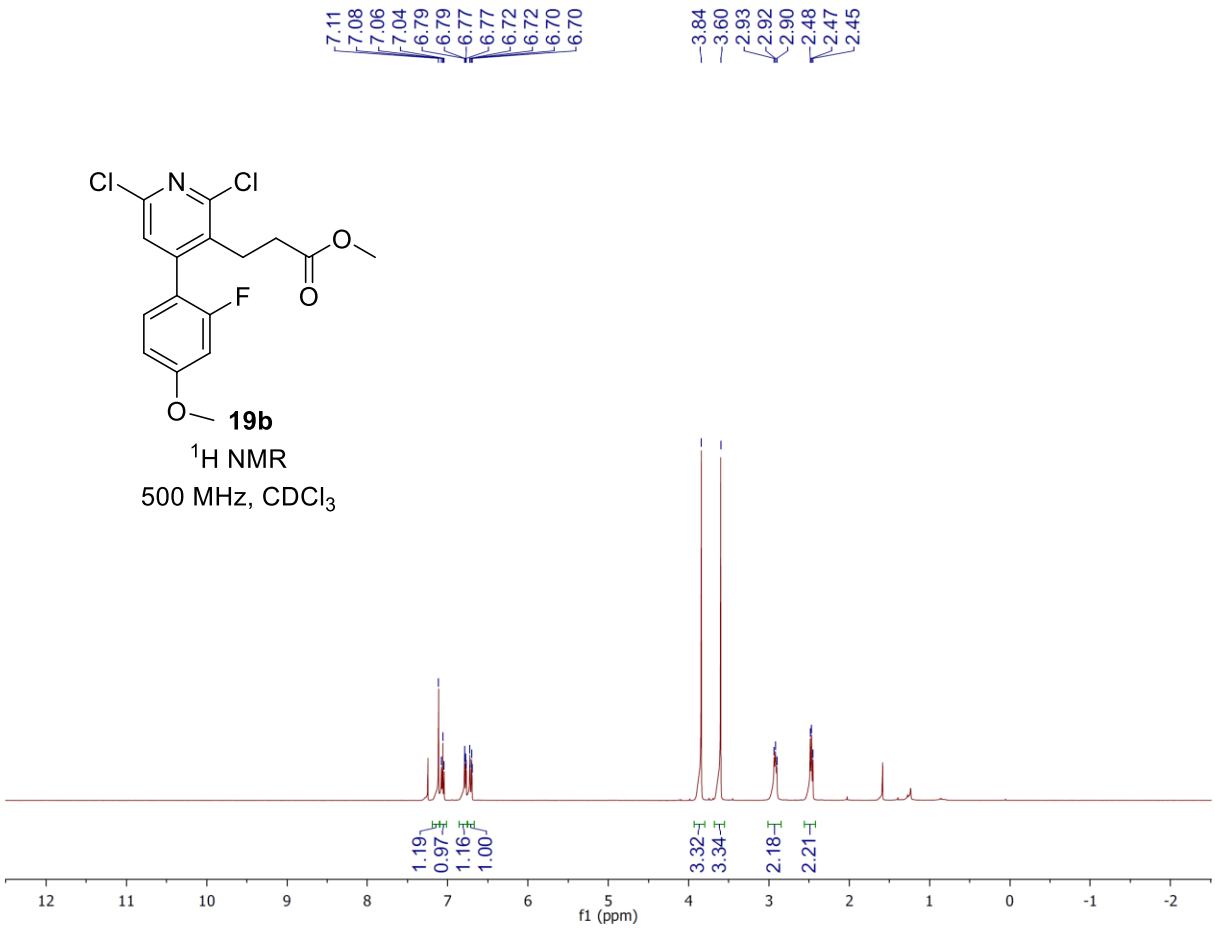
7.11
7.08
7.06
7.04
6.79
6.79
6.77
6.77
6.72
6.72
6.70
6.70
3.84
3.60
2.93
2.92
2.90
2.48
2.47
2.45
Cl
N
Cl
O
O
F
O
19b
1H NMR
500 MHz, CDCl3
1.19
0.97
1.16
1.00
3.32
3.34
2.18
2.21
12
11
10
9
8
7
6
5
4
3
2
1
0
-1
-2
f1 (ppm)

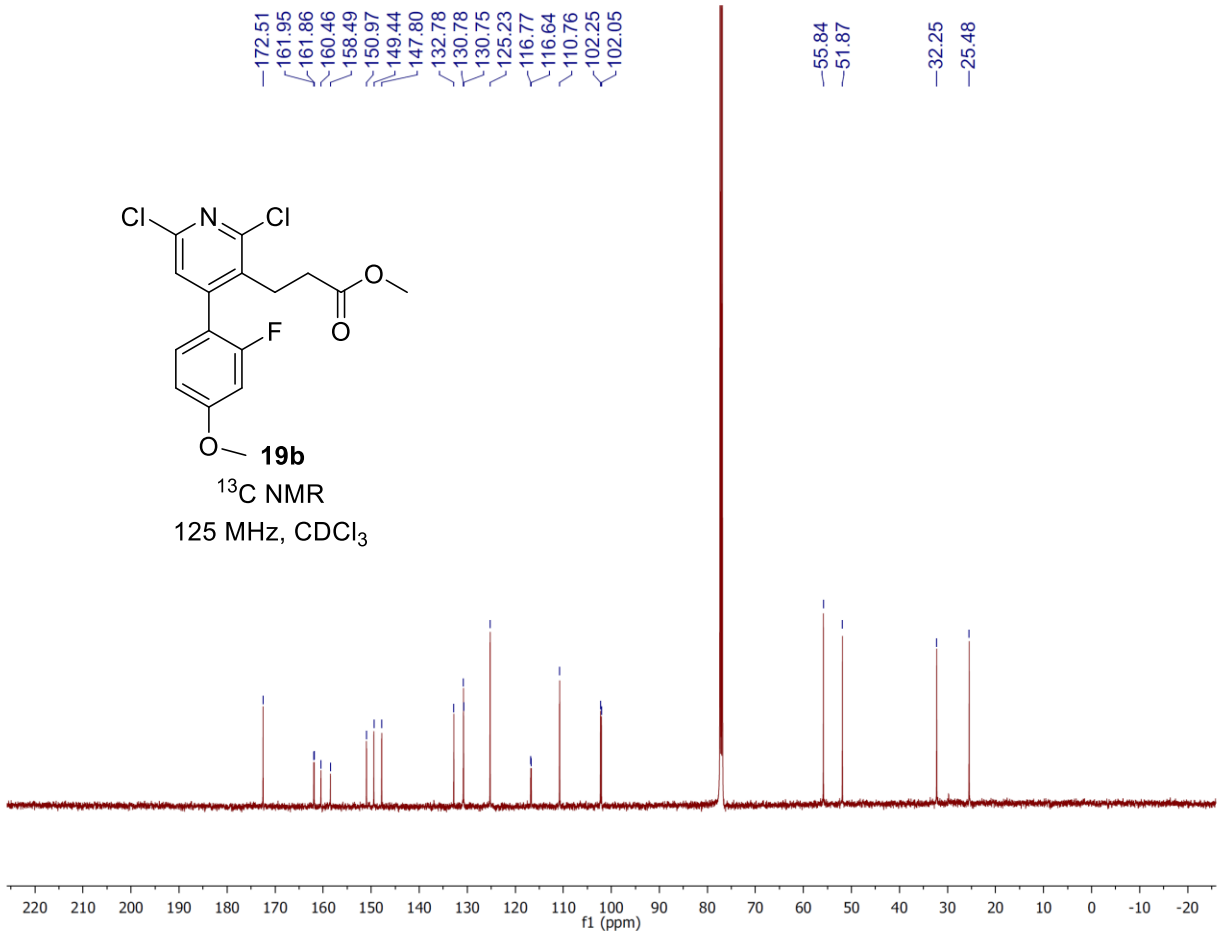
172.51
161.95
161.86
160.46
158.49
150.97
149.44
147.80
132.78
130.78
130.75
125.23
116.77
116.64
110.76
102.25
102.05
55.84
51.87
32.25
25.48
Cl
N
Cl
O
O
F
O
19b
13C NMR
125 MHz, CDCl3
220 210 200 190 180 170 160 150 140 130 120 110 100 90 80 70 60 50 40 30 20 10 0 -10 -20
f1 (ppm)

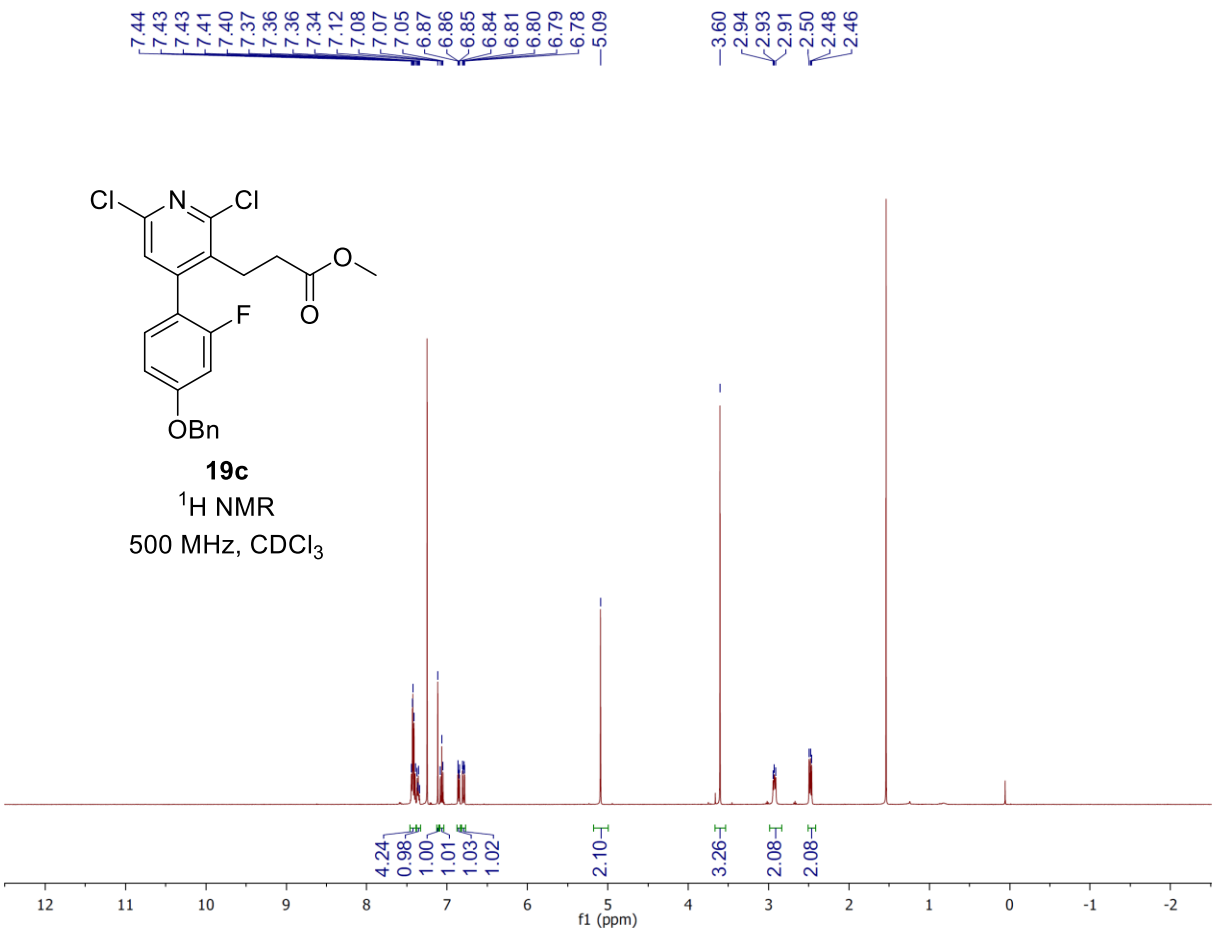
7.44
7.43
7.43
7.41
7.40
7.37
7.36
7.36
7.34
7.12
7.08
7.07
7.05
6.87
6.86
6.85
6.84
6.81
6.80
6.79
6.78
5.09
3.60
2.94
2.93
2.91
2.50
2.48
2.46
Cl
N
Cl
O
O
F
OBn
19c
1H NMR
500 MHz, CDCl3
4.24
0.98
1.00
1.01
1.03
1.02
2.10
3.26
2.08
2.08
12
11
10
9
8
7
6
5
4
3
2
1
0
-1
-2
f1 (ppm)

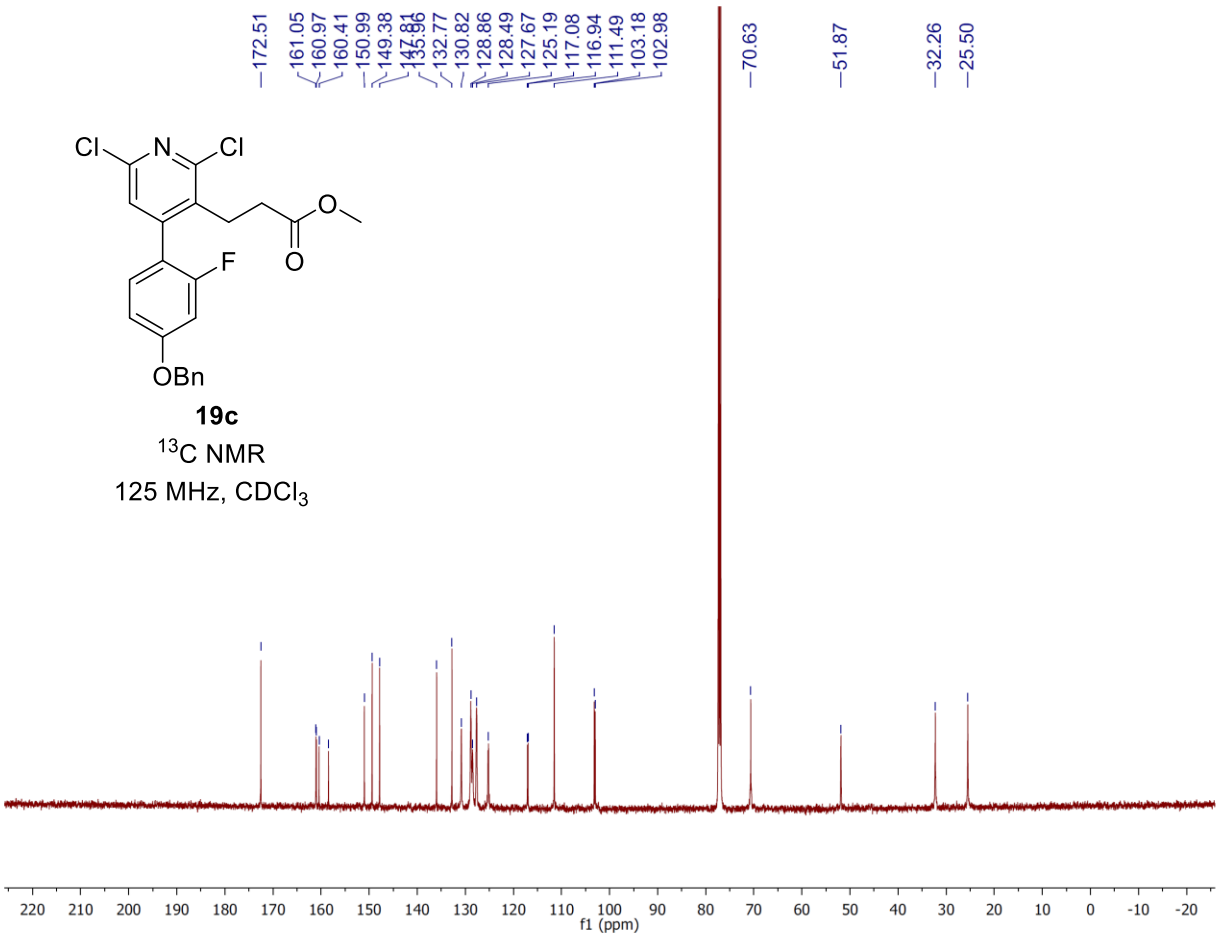
172.51
161.05
160.97
160.41
150.99
149.38
132.77
130.82
128.86
128.49
127.67
125.19
117.08
116.94
111.49
103.18
102.98
70.63
51.87
32.26
25.50
Cl
N
Cl
O
O
F
OBn
19c
13C NMR
125 MHz, CDCl3
220 210 200 190 180 170 160 150 140 130 120 110 100 90 80 70 60 50 40 30 20 10 0 -10 -20
f1 (ppm)

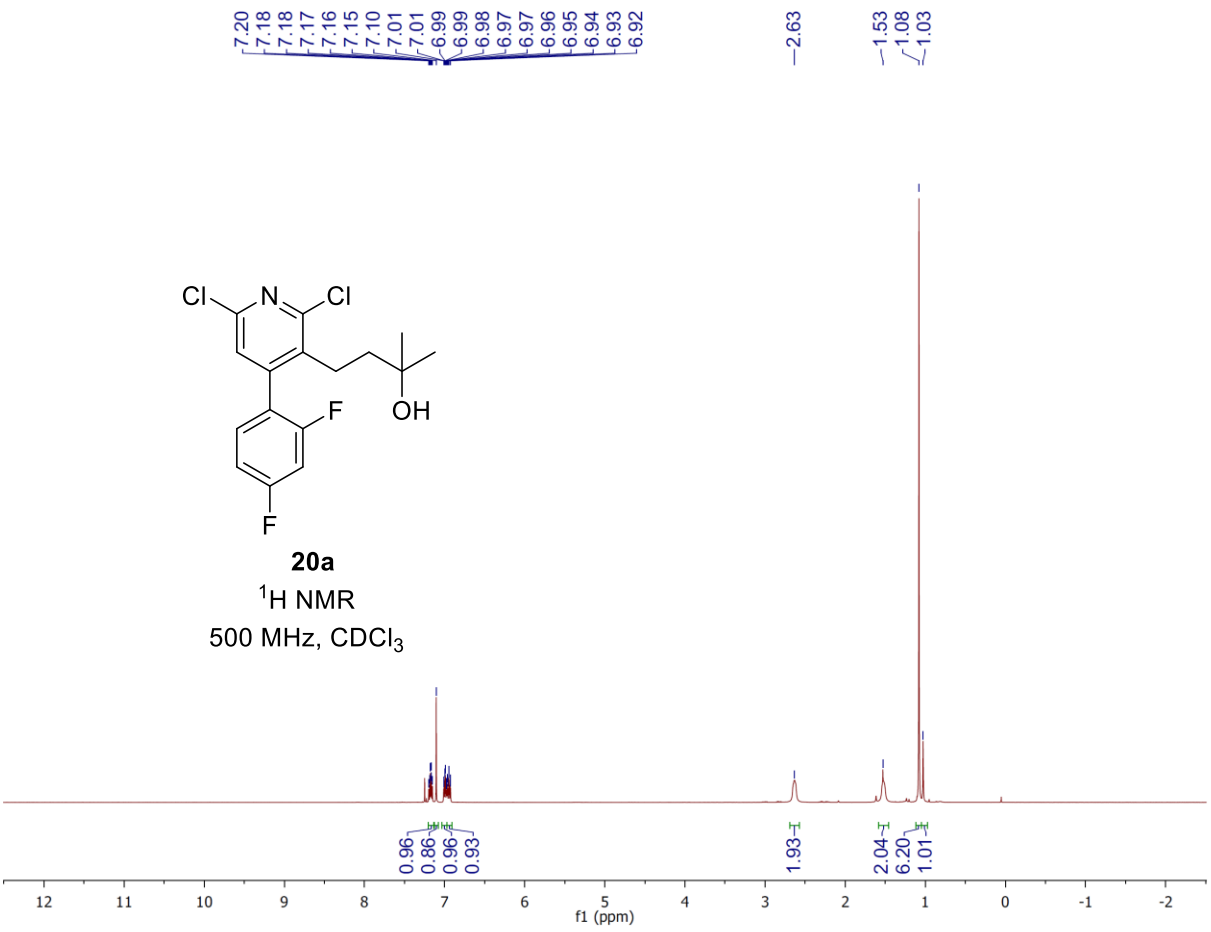

20a

^{1}H NMR

500 MHz, $CDCl_3$

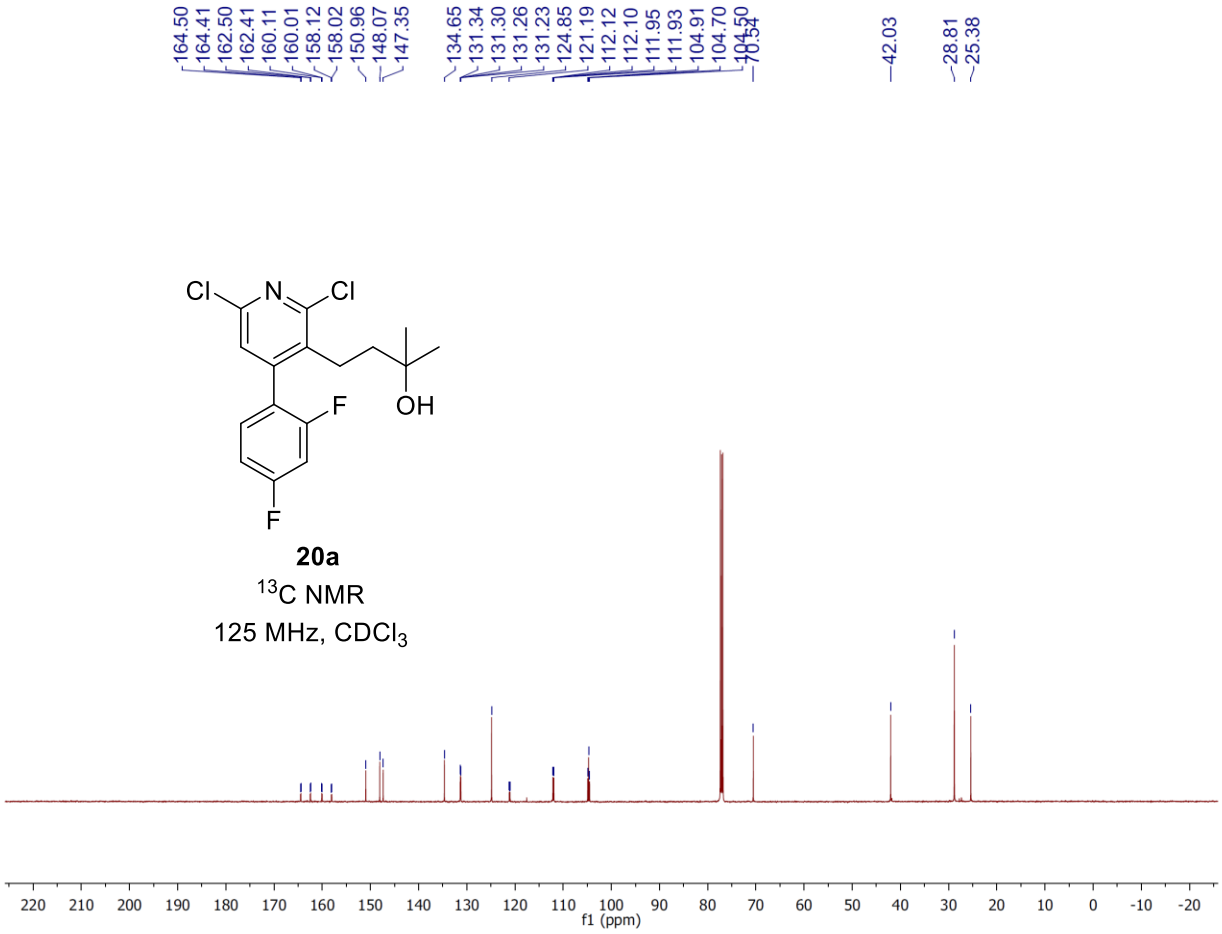
164.50
164.41
162.50
162.41
160.11
160.01
158.12
158.02
150.96
148.07
147.35
134.65
131.34
131.30
131.26
131.23
124.85
121.19
112.12
112.10
111.95
111.93
104.91
104.70
104.50
70.54
42.03
28.81
25.38
Cl
N
Cl
F
OH
F
20a
13C NMR
125 MHz, CDCl3
220 210 200 190 180 170 160 150 140 130 120 110 100 90 80 70 60 50 40 30 20 10 0 -10 -20
f1 (ppm)

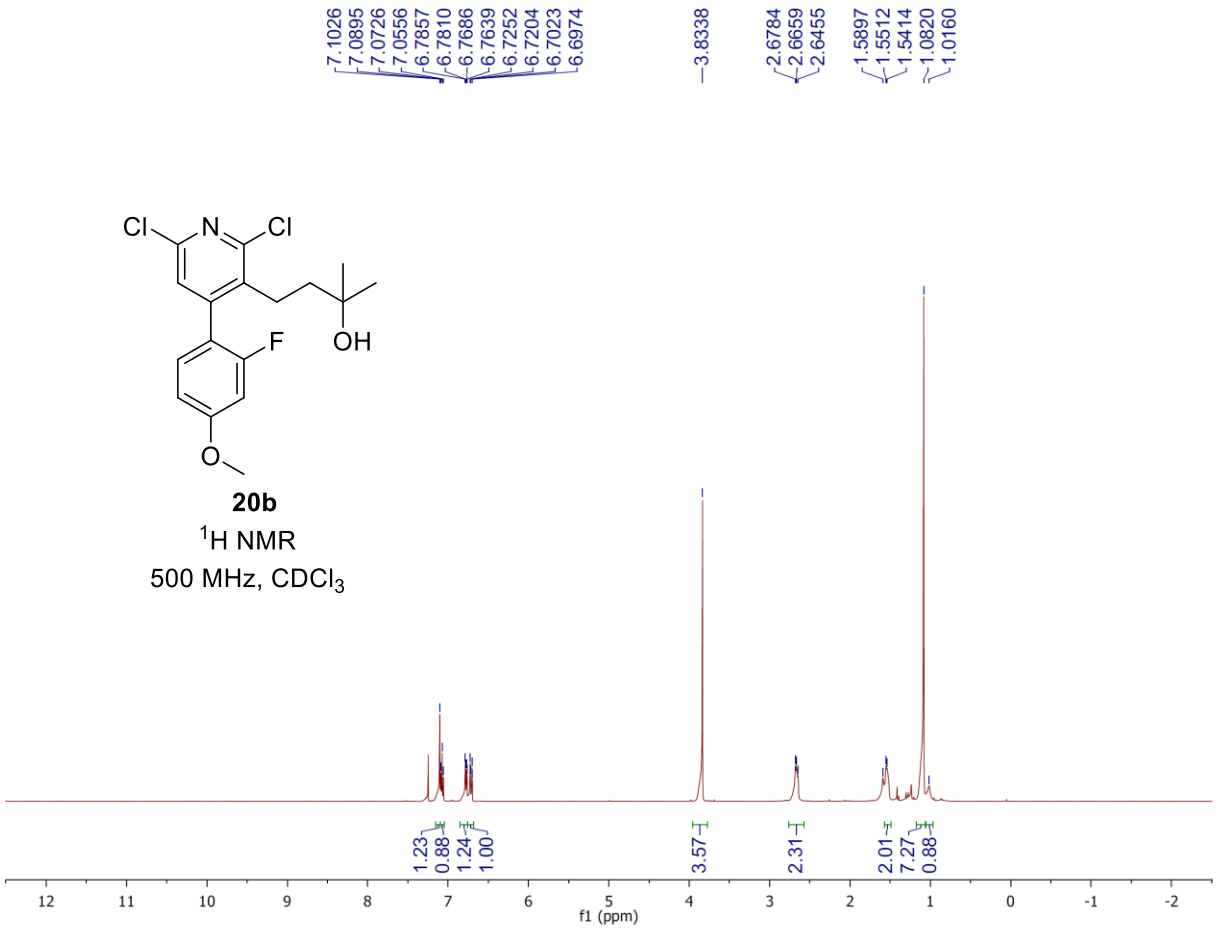
7.1026
7.0895
7.0726
7.0556
6.7857
6.7810
6.7686
6.7639
6.7252
6.7204
6.7023
6.6974
3.8338
2.6784
2.6659
2.6455
1.5897
1.5512
1.5414
1.0820
1.0160
Cl
N
Cl
F
OH
O
20b
1H NMR
500 MHz, CDCl3
1.23
0.88
1.24
1.00
3.57
2.31
2.01
7.27
0.88
12
11
10
9
8
7
6
5
4
3
2
1
0
-1
-2
f1 (ppm)

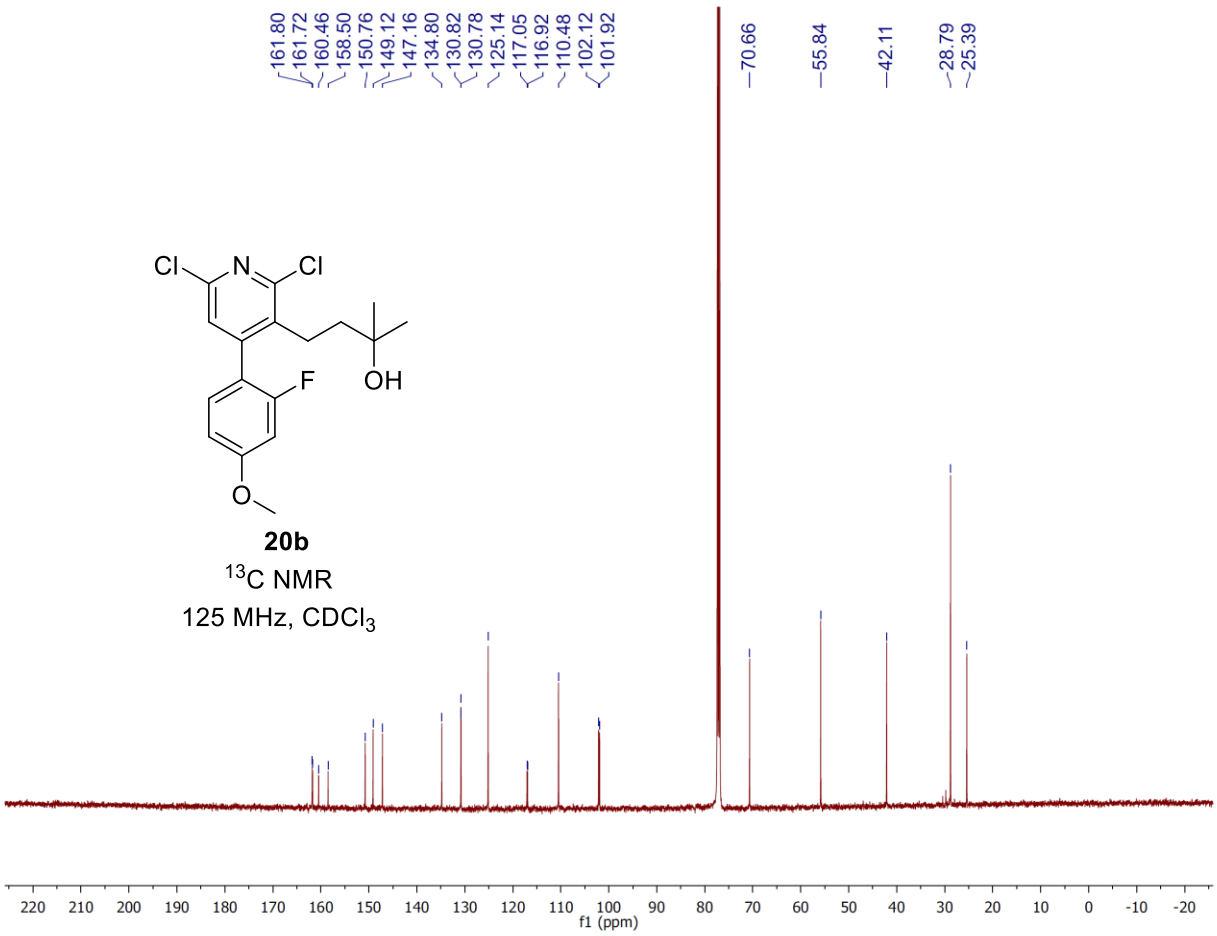
161.80
161.72
160.46
158.50
150.76
149.12
147.16
134.80
130.82
130.78
125.14
117.05
116.92
110.48
102.12
101.92
70.66
55.84
42.11
28.79
25.39
Cl
N
Cl
F
OH
O
20b
13C NMR
125 MHz, CDCl3
220 210 200 190 180 170 160 150 140 130 120 110 100 90 80 70 60 50 40 30 20 10 0 -10 -20
f1 (ppm)

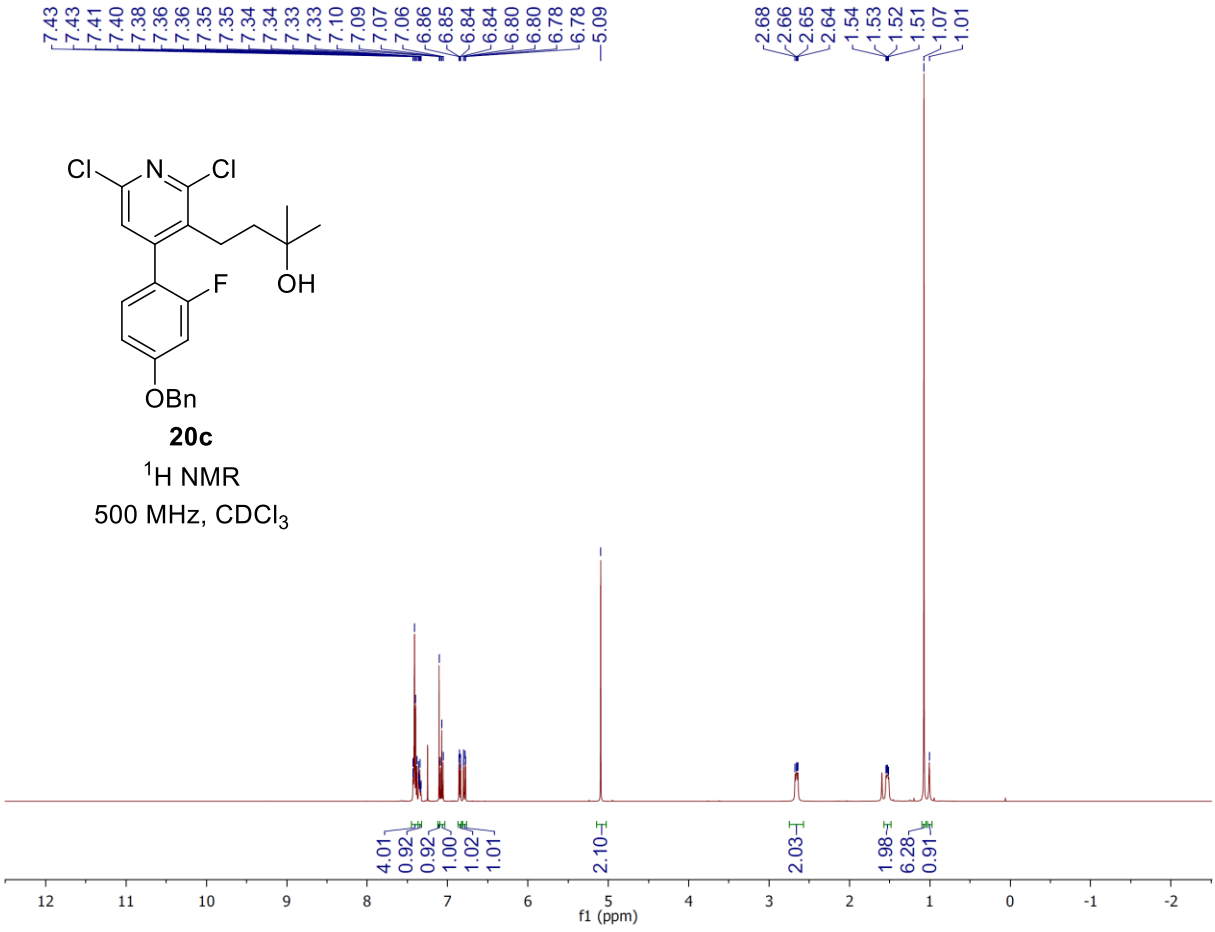

20c

^{1}H NMR

500 MHz, $CDCl_3$

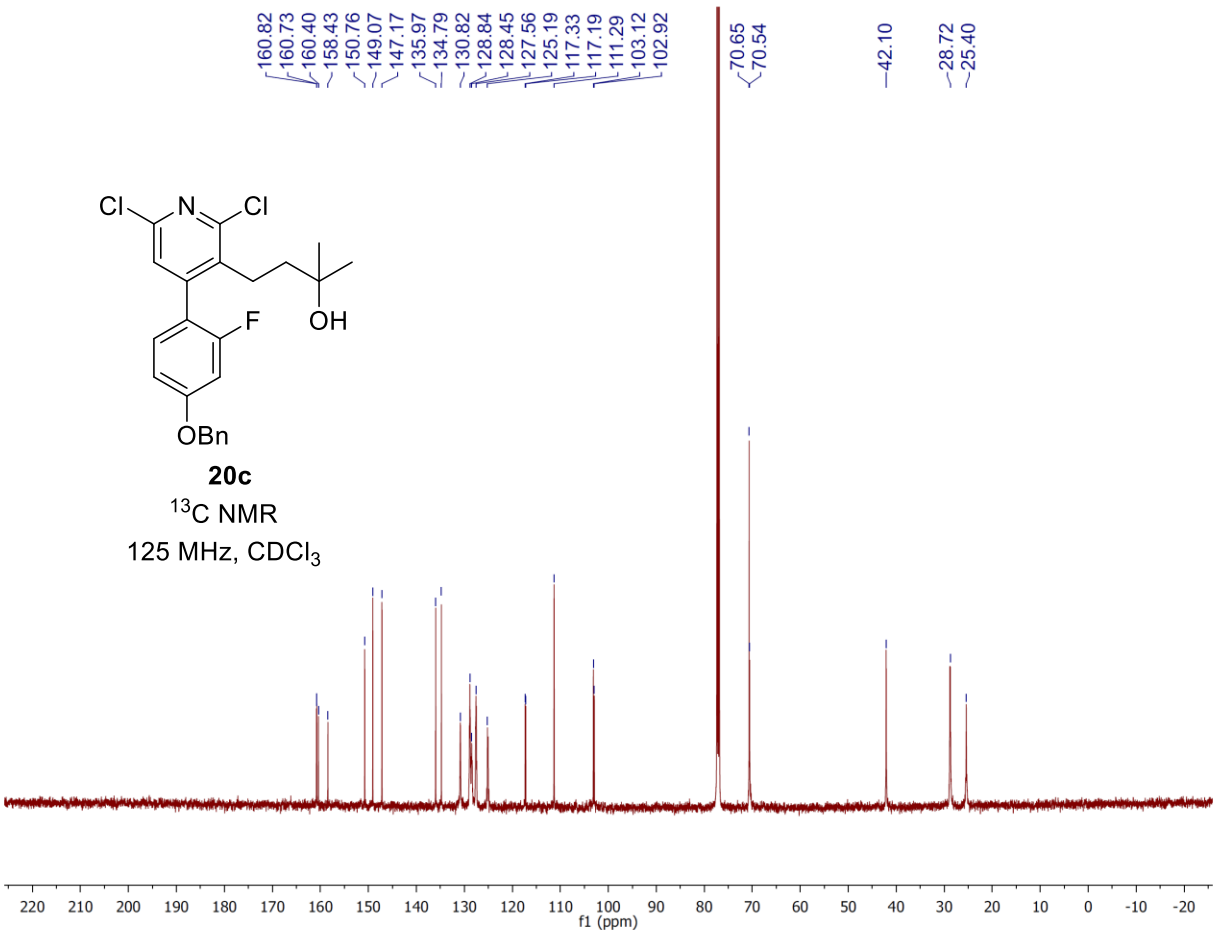
160.82
160.73
160.40
158.43
150.76
149.07
147.17
135.97
134.79
130.82
128.84
128.45
127.56
125.19
117.33
117.19
111.29
103.12
102.92
70.65
70.54
42.10
28.72
25.40
Cl
N
Cl
F
OH
OBn
20c
13C NMR
125 MHz, CDCl3
220 210 200 190 180 170 160 150 140 130 120 110 100 90 80 70 60 50 40 30 20 10 0 -10 -20
f1 (ppm)

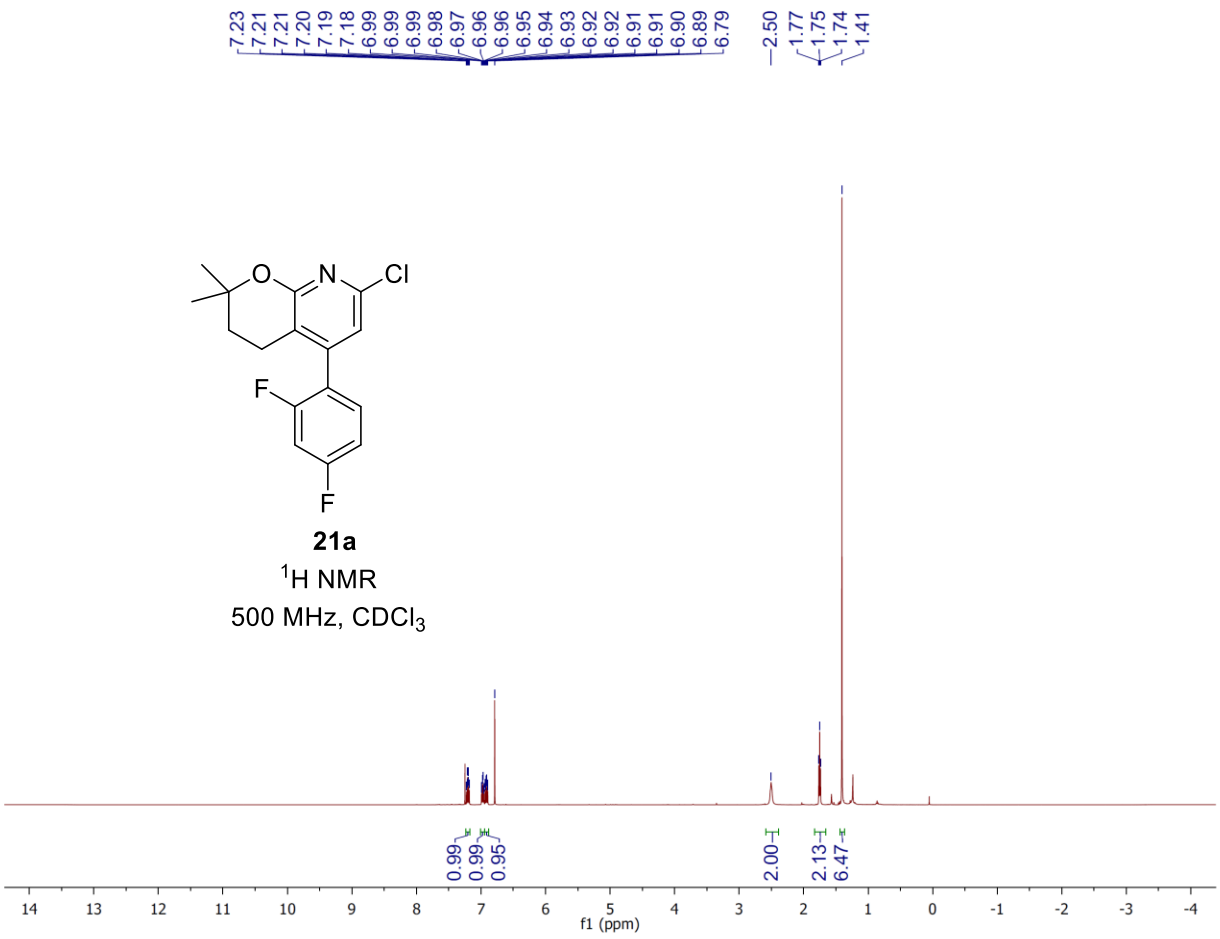
7.23
7.21
7.21
7.20
7.19
7.18
6.99
6.99
6.99
6.98
6.97
6.96
6.96
6.95
6.94
6.93
6.92
6.92
6.91
6.91
6.90
6.89
6.79
2.50
1.77
1.75
1.74
1.41
O
N
Cl
F
F
21a
1H NMR
500 MHz, CDCl3
0.99
0.99
0.95
2.00
2.13
6.47
14
13
12
11
10
9
8
7
6
5
4
3
2
1
0
-1
-2
-3
-4
f1 (ppm)

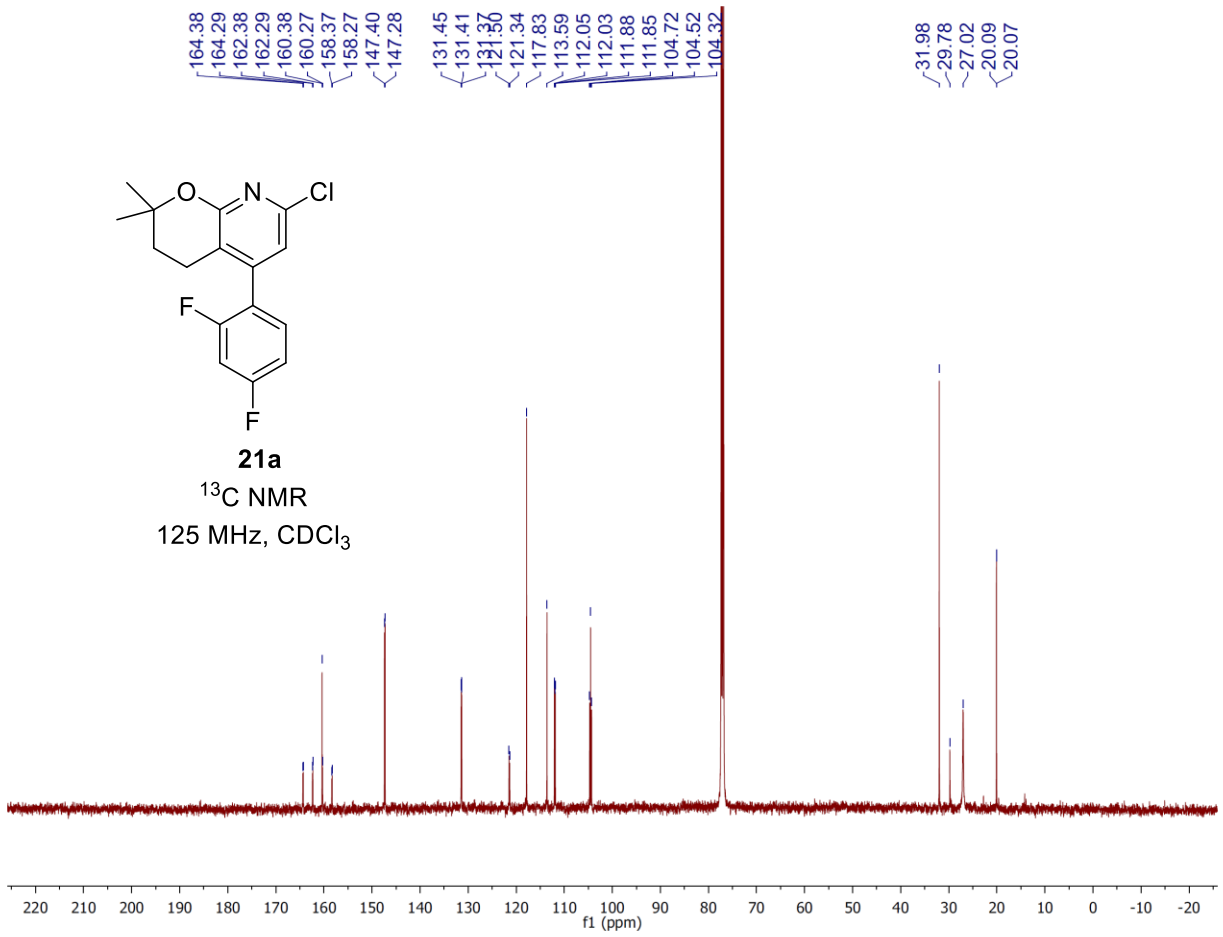
164.38
164.29
162.38
162.29
160.38
160.27
158.37
158.27
147.40
147.28
131.45
131.41
121.34
117.83
113.59
112.05
112.03
111.88
111.85
104.72
104.52
104.32
31.98
29.78
27.02
20.09
20.07
O
N
Cl
F
F
21a
13C NMR
125 MHz, CDCl3
220 210 200 190 180 170 160 150 140 130 120 110 100 90 80 70 60 50 40 30 20 10 0 -10 -20
f1 (ppm)

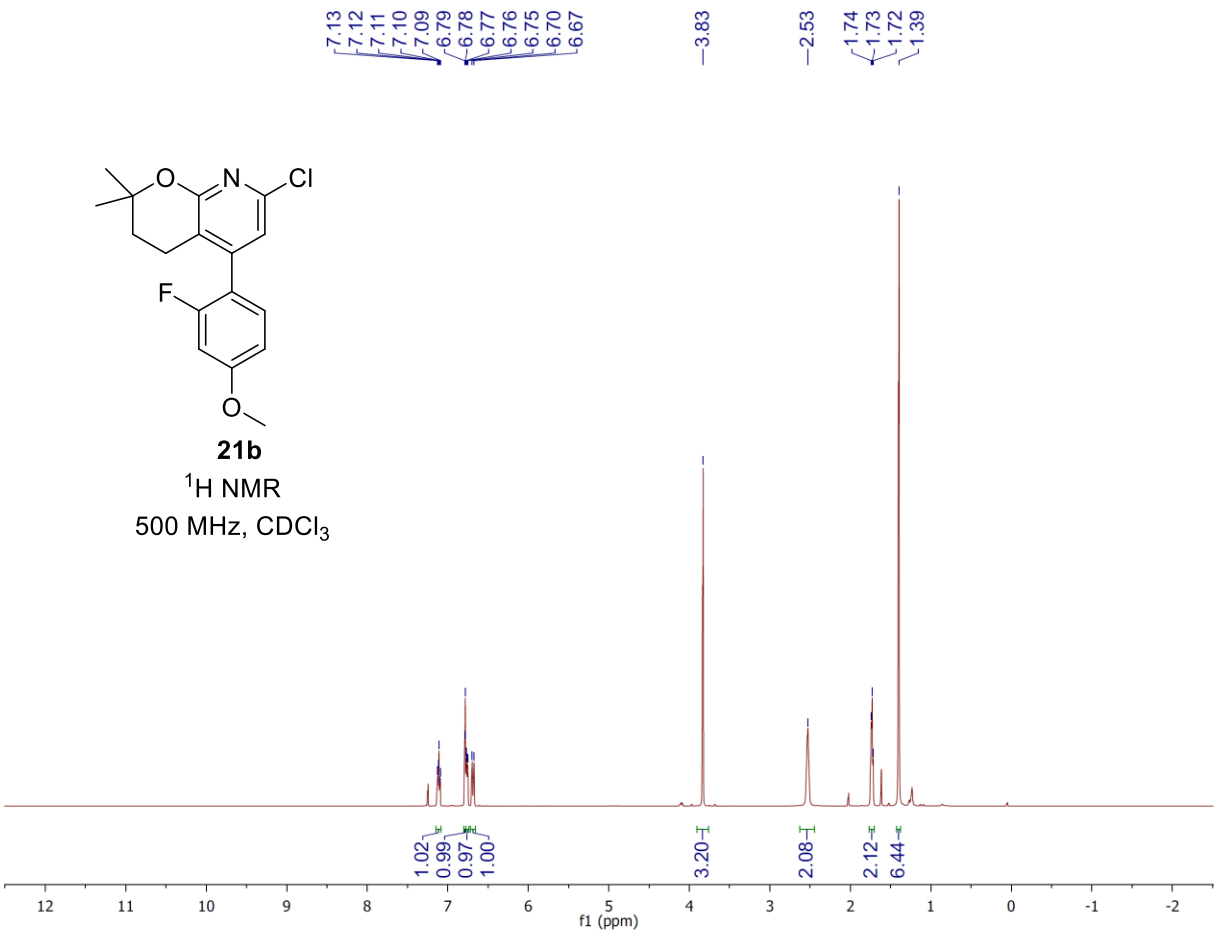
7.13
7.12
7.11
7.10
7.09
6.79
6.78
6.77
6.76
6.75
6.70
6.67
3.83
2.53
1.74
1.73
1.72
1.39
O
N
Cl
F
O
21b
1H NMR
500 MHz, CDCl3
1.02
0.99
0.97
1.00
3.20
2.08
2.12
6.44
12
11
10
9
8
7
6
5
4
3
2
1
0
-1
-2
f1 (ppm)

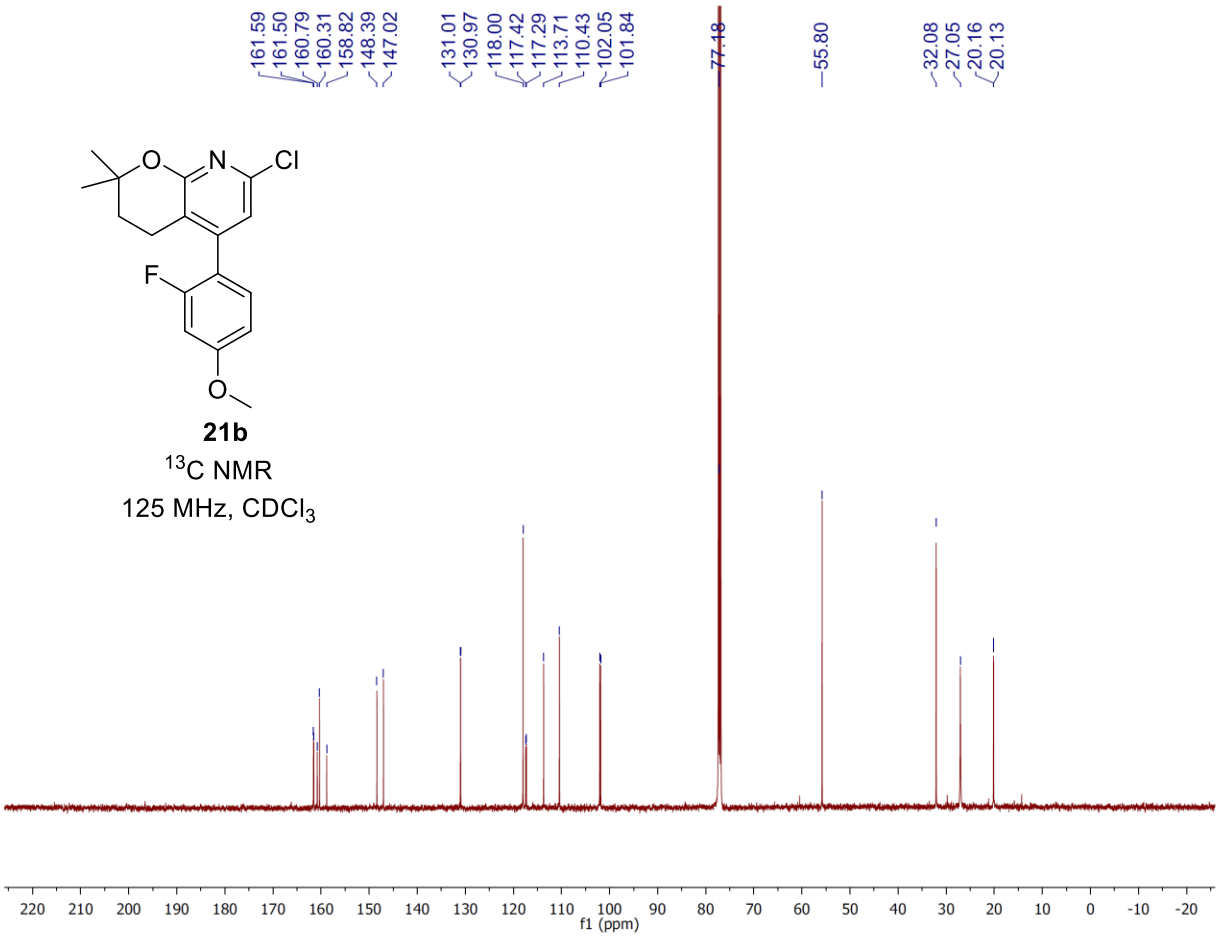
161.59
161.50
160.79
160.31
158.82
148.39
147.02
131.01
130.97
118.00
117.42
117.29
113.71
110.43
102.05
101.84
77.48
55.80
32.08
27.05
20.16
20.13
O
N
Cl
F
O
21b
13C NMR
125 MHz, CDCl3
220 210 200 190 180 170 160 150 140 130 120 110 100 90 80 70 60 50 40 30 20 10 0 -10 -20
f1 (ppm)

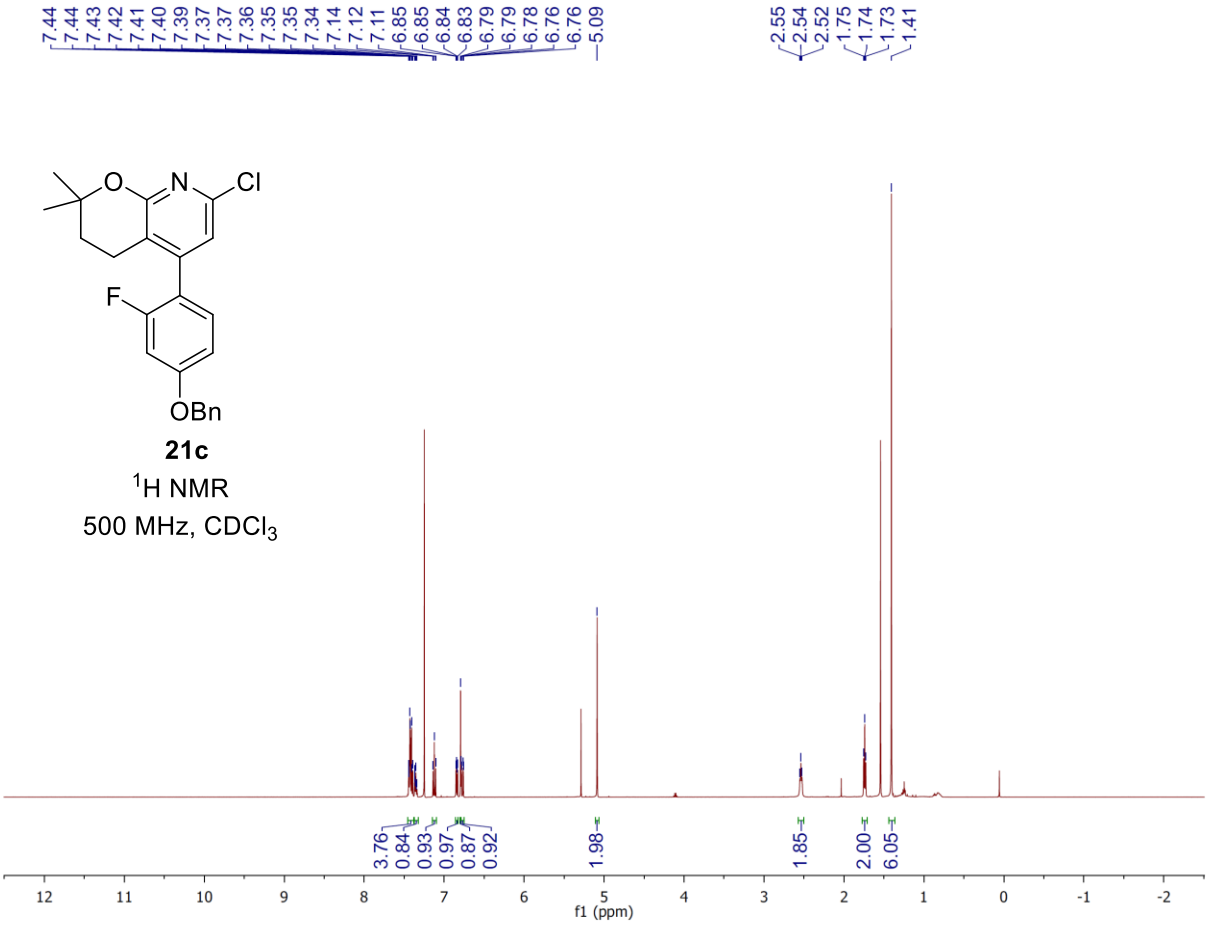
7.44
7.44
7.43
7.42
7.41
7.40
7.39
7.37
7.37
7.36
7.35
7.35
7.34
7.14
7.12
7.11
6.85
6.85
6.84
6.83
6.79
6.79
6.78
6.76
6.76
5.09
2.55
2.54
2.52
1.75
1.74
1.73
1.41
O
N
Cl
F
OBn
21c
1H NMR
500 MHz, CDCl3
3.76
0.84
0.93
0.97
0.87
0.92
1.98
1.85
2.00
6.05
12
11
10
9
8
7
6
5
4
3
2
1
0
-1
-2
f1 (ppm)

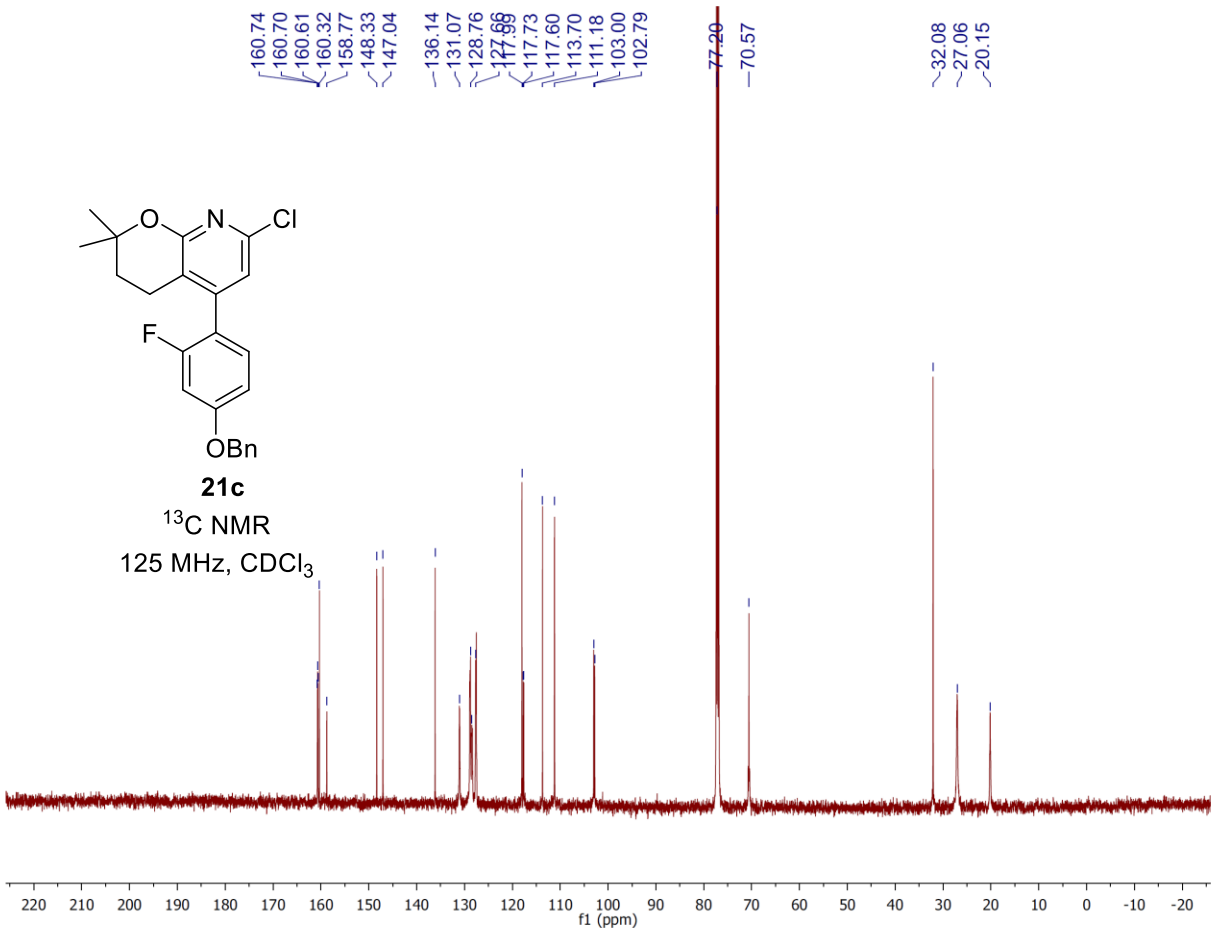
160.74
160.70
160.61
160.32
158.77
148.33
147.04
136.14
131.07
128.76
117.73
117.60
113.70
111.18
103.00
102.79
77.20
70.57
32.08
27.06
20.15
O
N
Cl
F
OBn
21c
13C NMR
125 MHz, CDCl3
220 210 200 190 180 170 160 150 140 130 120 110 100 90 80 70 60 50 40 30 20 10 0 -10 -20
f1 (ppm)

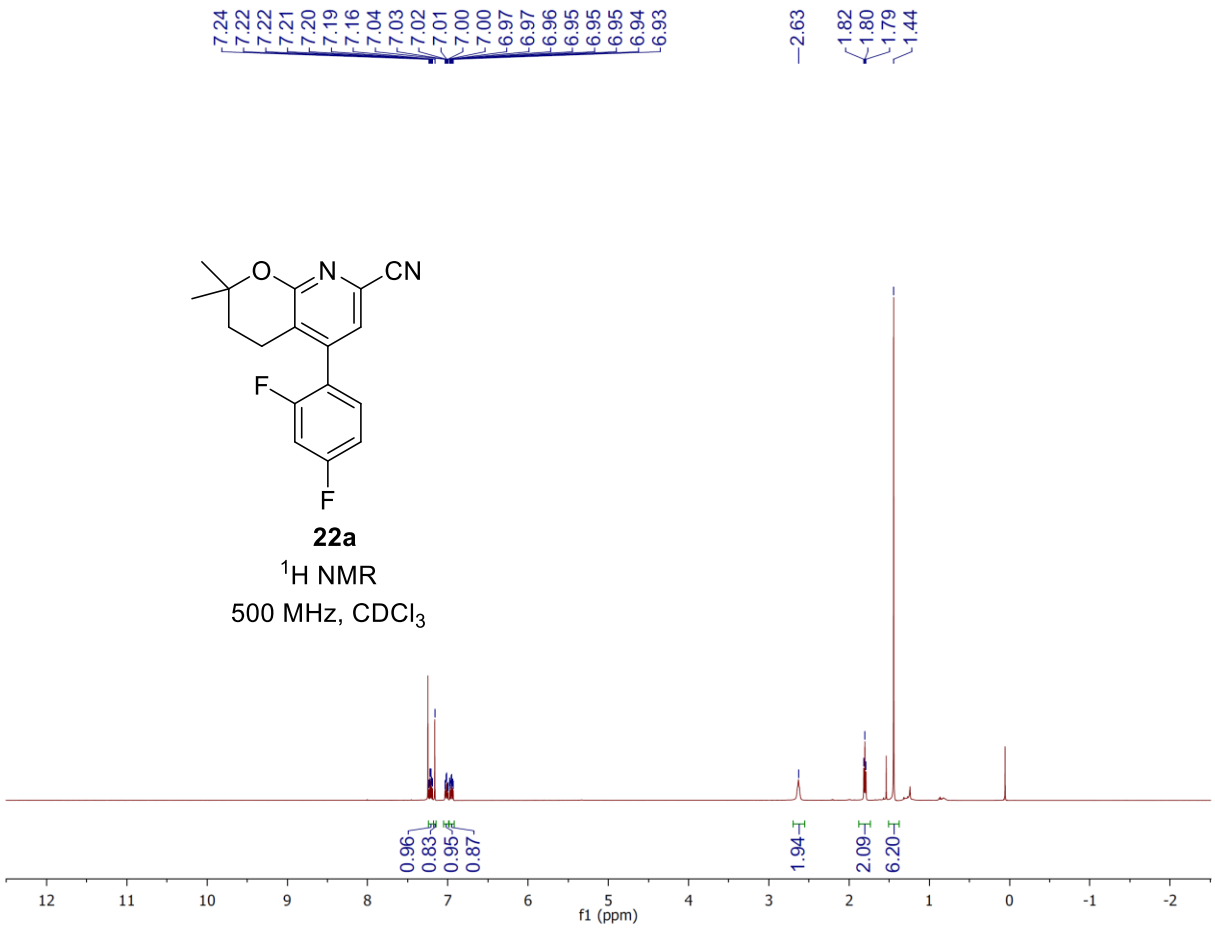

22a

^{1}H NMR

500 MHz, $CDCl_3$

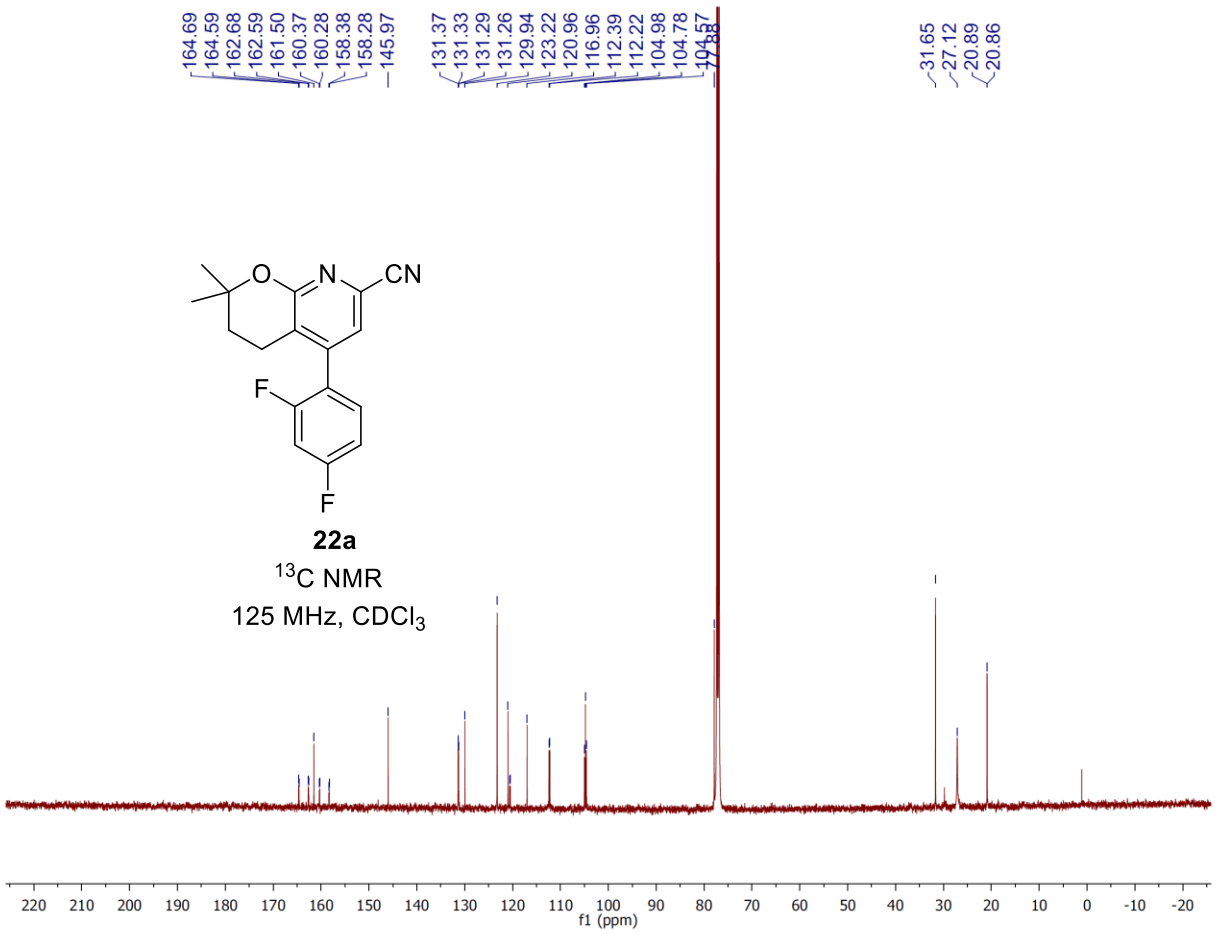
164.69
164.59
162.68
162.59
161.50
160.37
160.28
158.38
158.28
145.97
131.37
131.33
131.29
131.26
129.94
123.22
120.96
116.96
112.39
112.22
104.98
104.78
104.57
77.88
31.65
27.12
20.89
20.86
O
N
CN
F
F
22a
13C NMR
125 MHz, CDCl3
220 210 200 190 180 170 160 150 140 130 120 110 100 90 80 70 60 50 40 30 20 10 0 -10 -20
f1 (ppm)

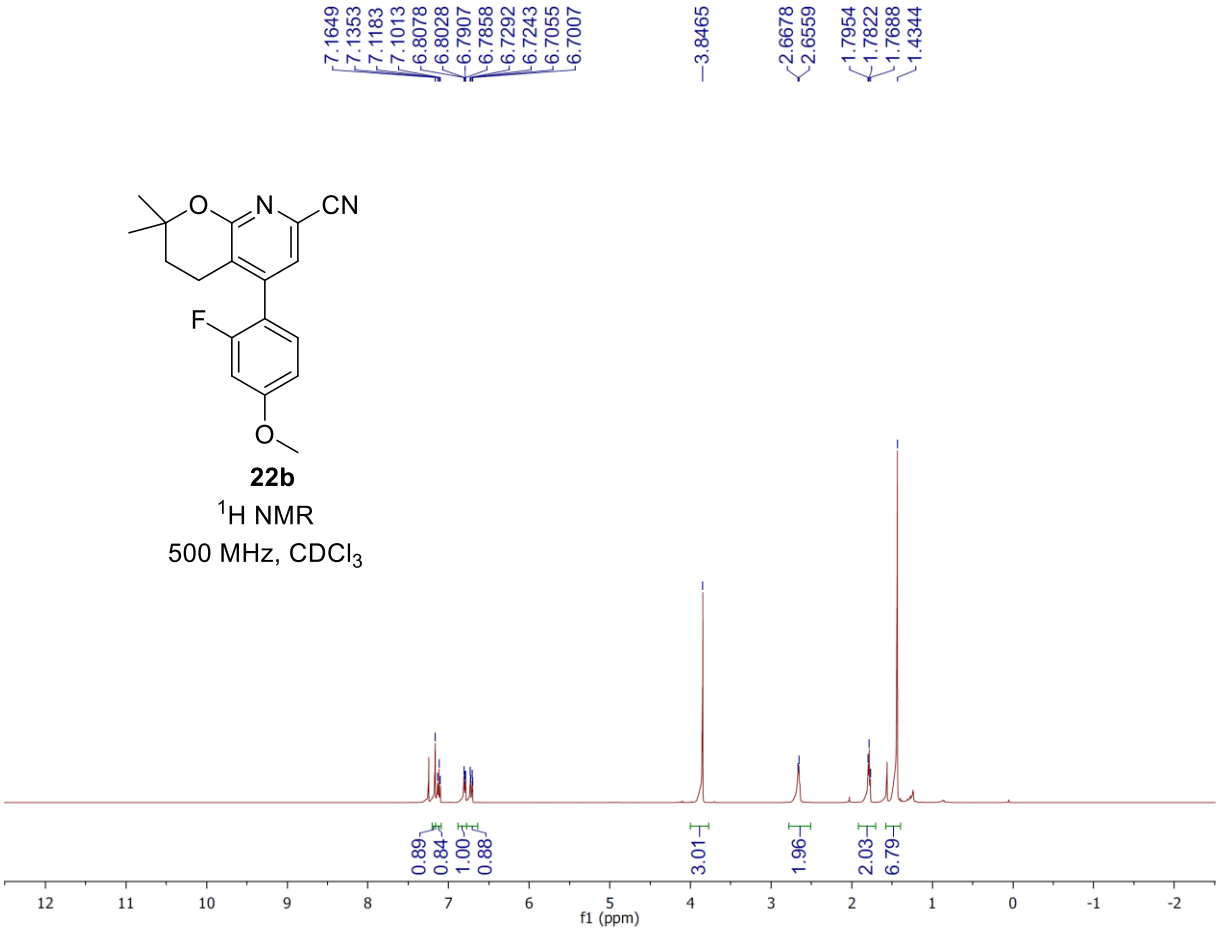
7.1649
7.1353
7.1183
7.1013
6.8078
6.8028
6.7907
6.7858
6.7292
6.7243
6.7055
6.7007
3.8465
2.6678
2.6559
1.7954
1.7822
1.7688
1.4344
O
N
CN
F
O
22b
1H NMR
500 MHz, CDCl3
0.89
0.84
1.00
0.88
3.01
1.96
2.03
6.79
12
11
10
9
8
7
6
5
4
3
2
1
0
-1
-2
f1 (ppm)

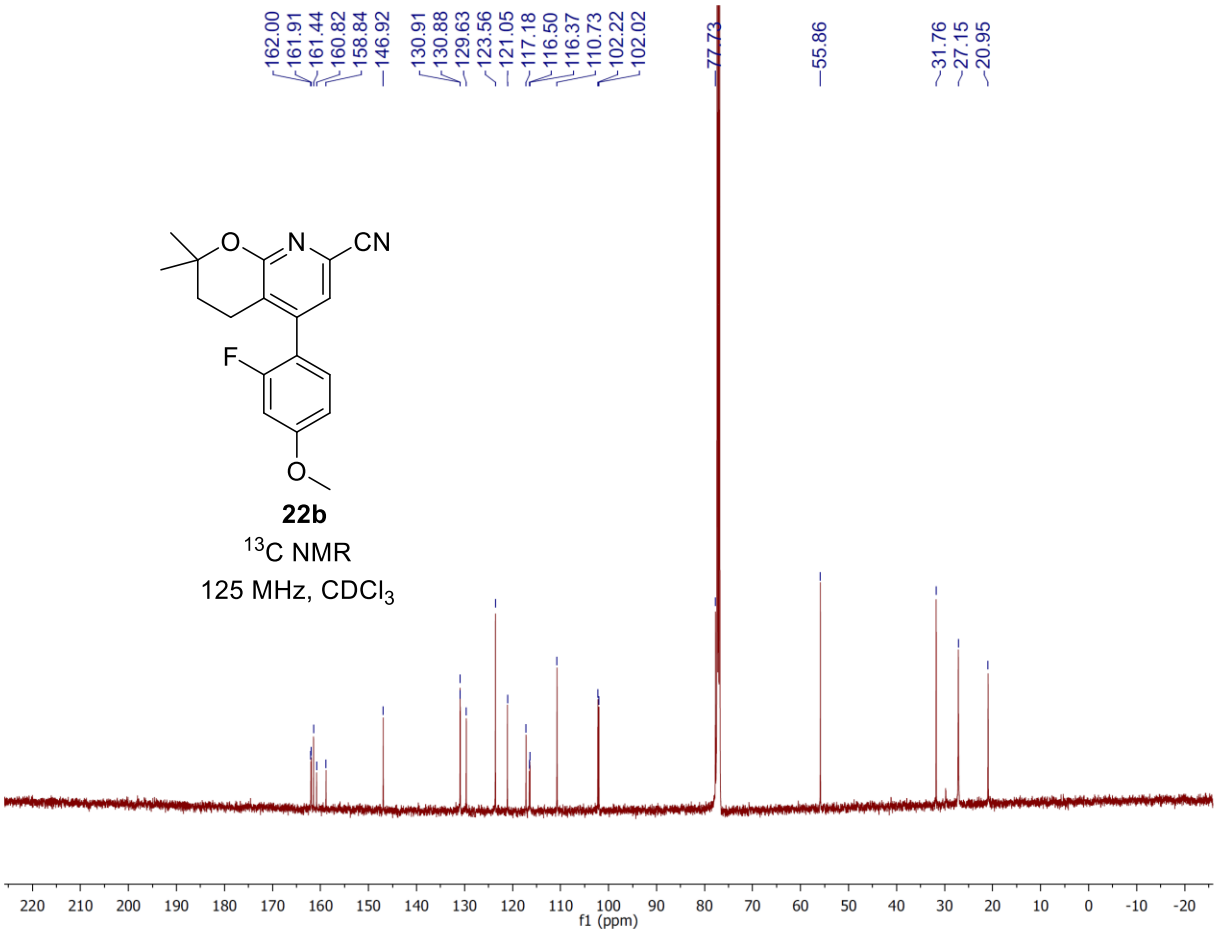
162.00
161.91
161.44
160.82
158.84
146.92
130.91
130.88
129.63
123.56
121.05
117.18
116.50
116.37
110.73
102.22
102.02
77.73
55.86
31.76
27.15
20.95
O
N
CN
F
O
22b
13C NMR
125 MHz, CDCl3
220 210 200 190 180 170 160 150 140 130 120 110 100 90 80 70 60 50 40 30 20 10 0 -10 -20
f1 (ppm)

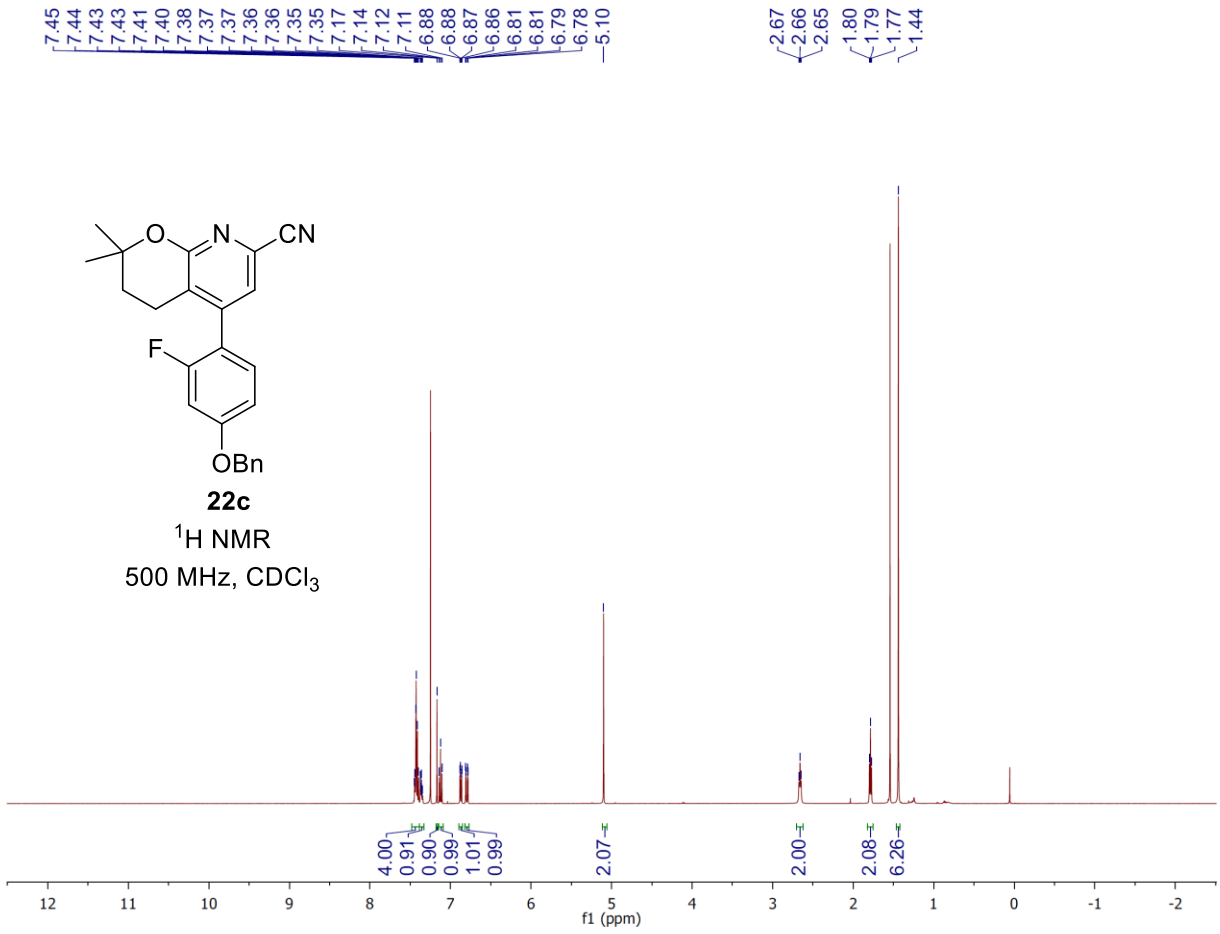
7.45
7.44
7.43
7.43
7.41
7.40
7.38
7.37
7.37
7.36
7.36
7.35
7.35
7.17
7.14
7.12
7.11
6.88
6.88
6.87
6.86
6.81
6.81
6.79
6.78
5.10
2.67
2.66
2.65
1.80
1.79
1.77
1.44
O
N
CN
F
OBn
22c
1H NMR
500 MHz, CDCl3
4.00
0.91
0.90
0.99
1.01
0.99
2.07
2.00
2.08
6.26
12
11
10
9
8
7
6
5
4
3
2
1
0
-1
-2
f1 (ppm)

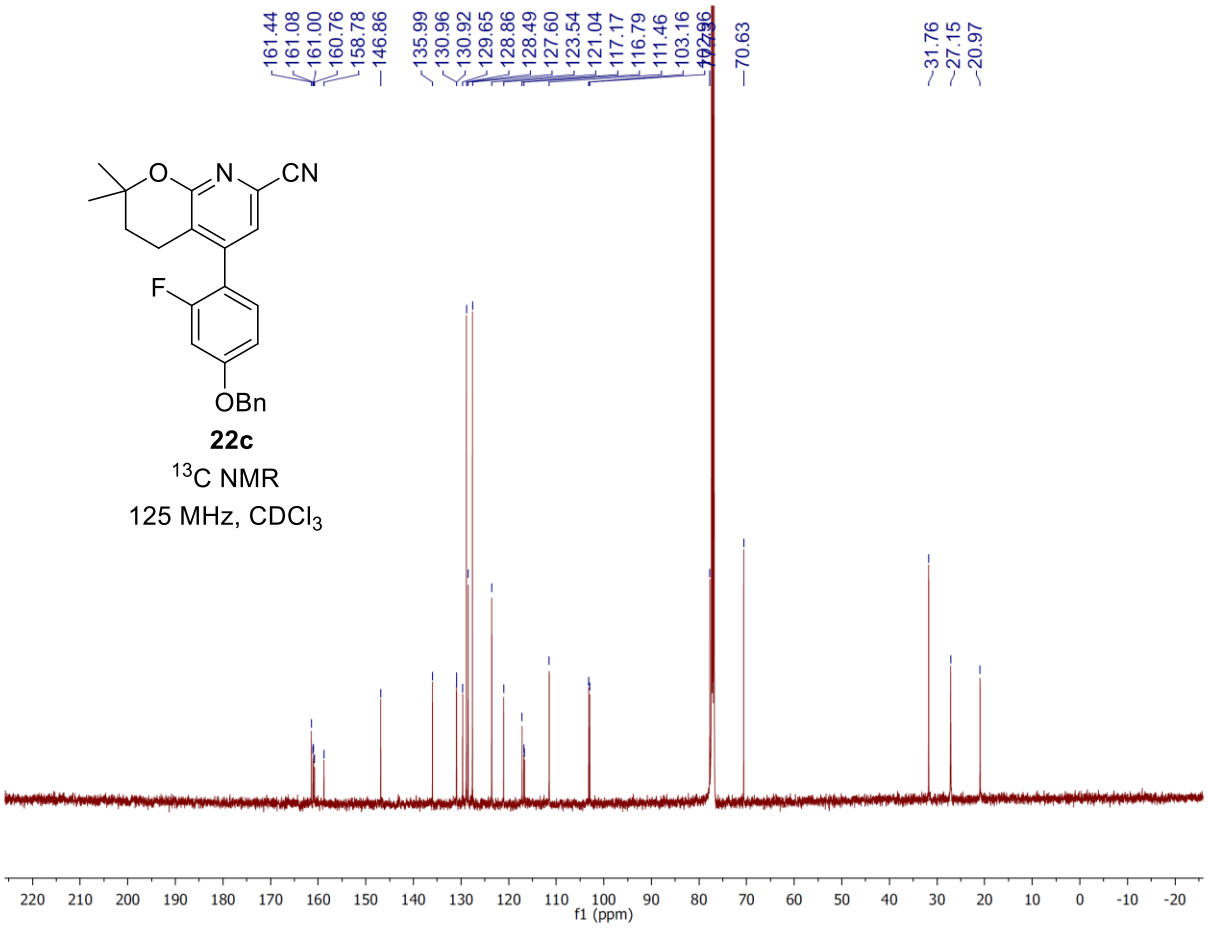
161.44
161.08
161.00
160.76
158.78
146.86
135.99
130.96
130.92
129.65
128.86
128.49
127.60
123.54
121.04
117.17
116.79
111.46
103.16
70.63
31.76
27.15
20.97
O
N
CN
F
OBn
22c
13C NMR
125 MHz, CDCl3
220 210 200 190 180 170 160 150 140 130 120 110 100 90 80 70 60 50 40 30 20 10 0 -10 -20
f1 (ppm)

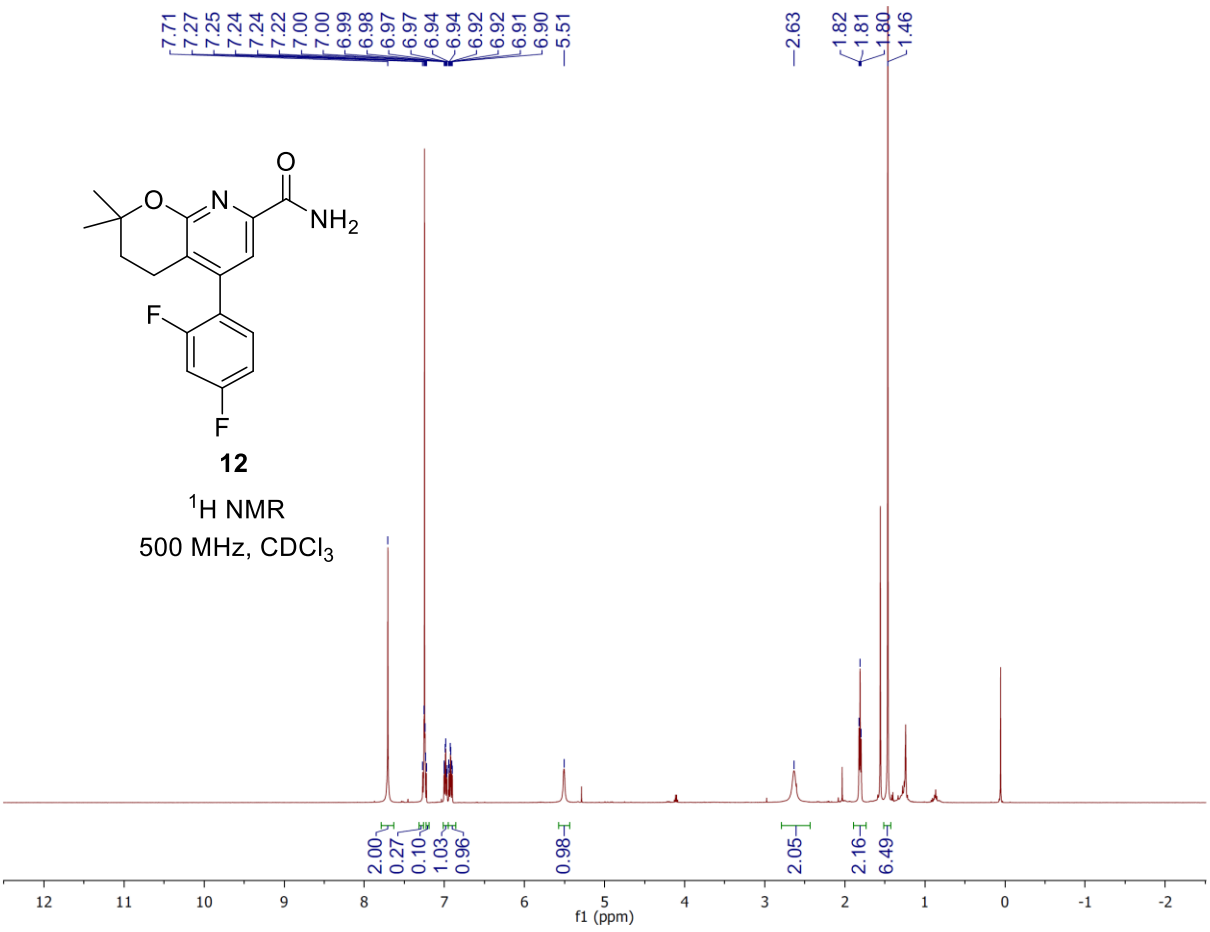
7.71
7.27
7.25
7.24
7.24
7.22
7.00
7.00
6.99
6.98
6.97
6.97
6.94
6.94
6.92
6.92
6.91
6.90
5.51
2.63
1.82
1.81
1.80
1.46
O
N
O
NH2
F
F
12
1H NMR
500 MHz, CDCl3
2.00
0.27
0.10
1.03
0.96
0.98
2.05
2.16
6.49
12
11
10
9
8
7
6
5
4
3
2
1
0
-1
-2
f1 (ppm)

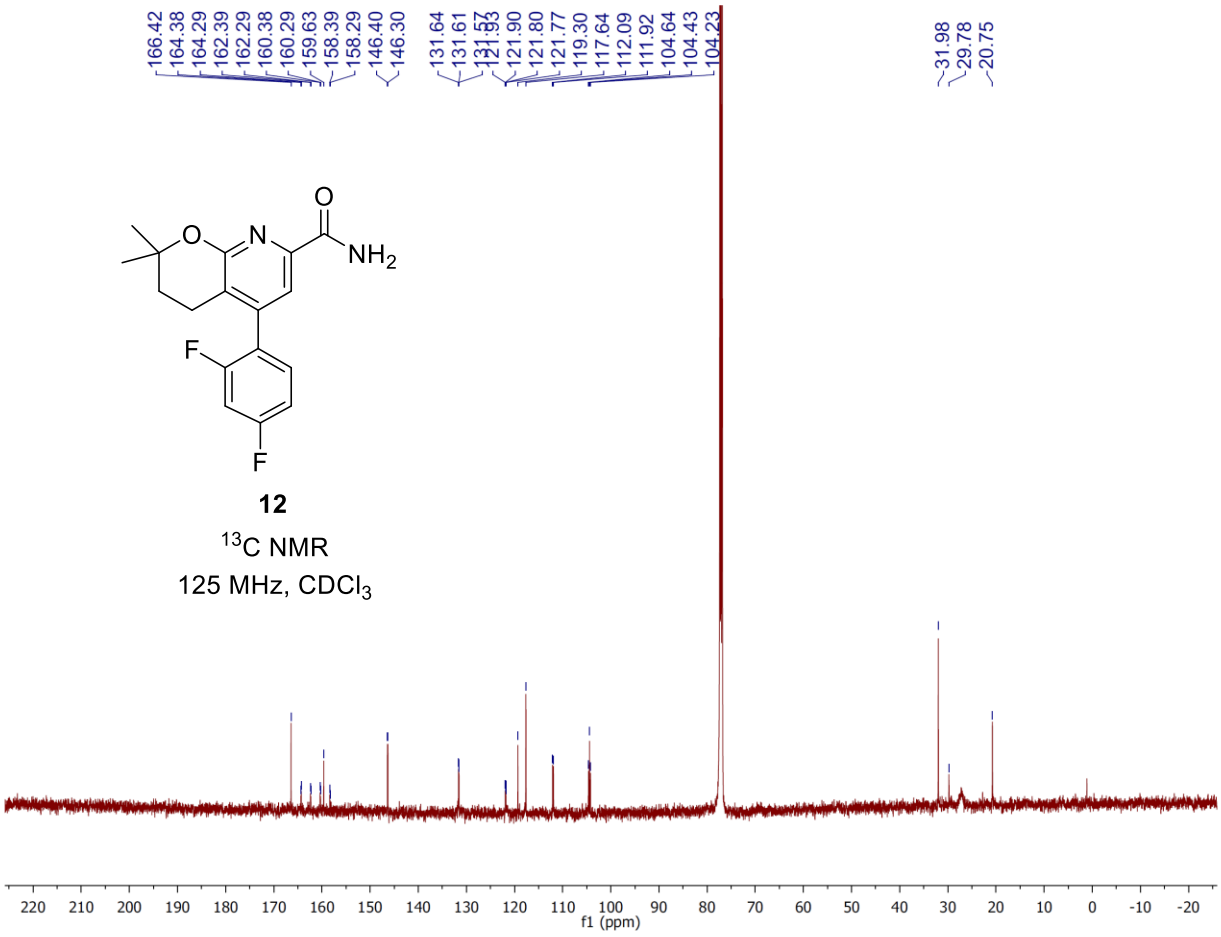
166.42
164.38
164.29
162.39
162.29
160.38
160.29
159.63
158.39
158.29
146.40
146.30
131.64
131.61
121.90
121.80
121.77
119.30
117.64
112.09
111.92
104.64
104.43
104.23
31.98
29.78
20.75
O
N
O
NH2
F
F
12
13C NMR
125 MHz, CDCl3
220 210 200 190 180 170 160 150 140 130 120 110 100 90 80 70 60 50 40 30 20 10 0 -10 -20
f1 (ppm)

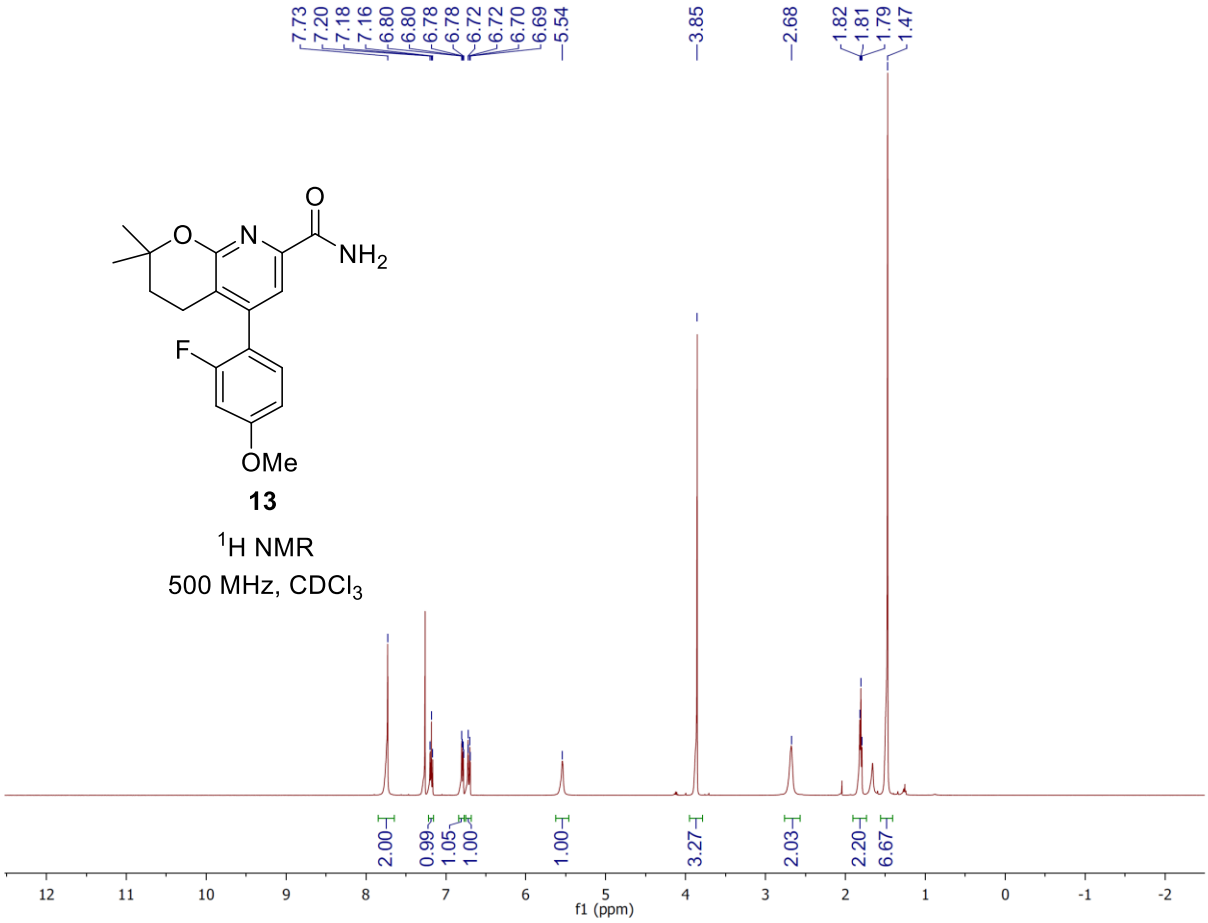
7.73
7.20
7.18
7.16
6.80
6.80
6.78
6.78
6.72
6.72
6.70
6.69
5.54
3.85
2.68
1.82
1.81
1.79
1.47
O
O
N
NH2
F
OMe
13
1H NMR
500 MHz, CDCl3
2.00
0.99
1.05
1.00
1.00
3.27
2.03
2.20
6.67
12
11
10
9
8
7
6
5
4
3
2
1
0
-1
-2
f1 (ppm)

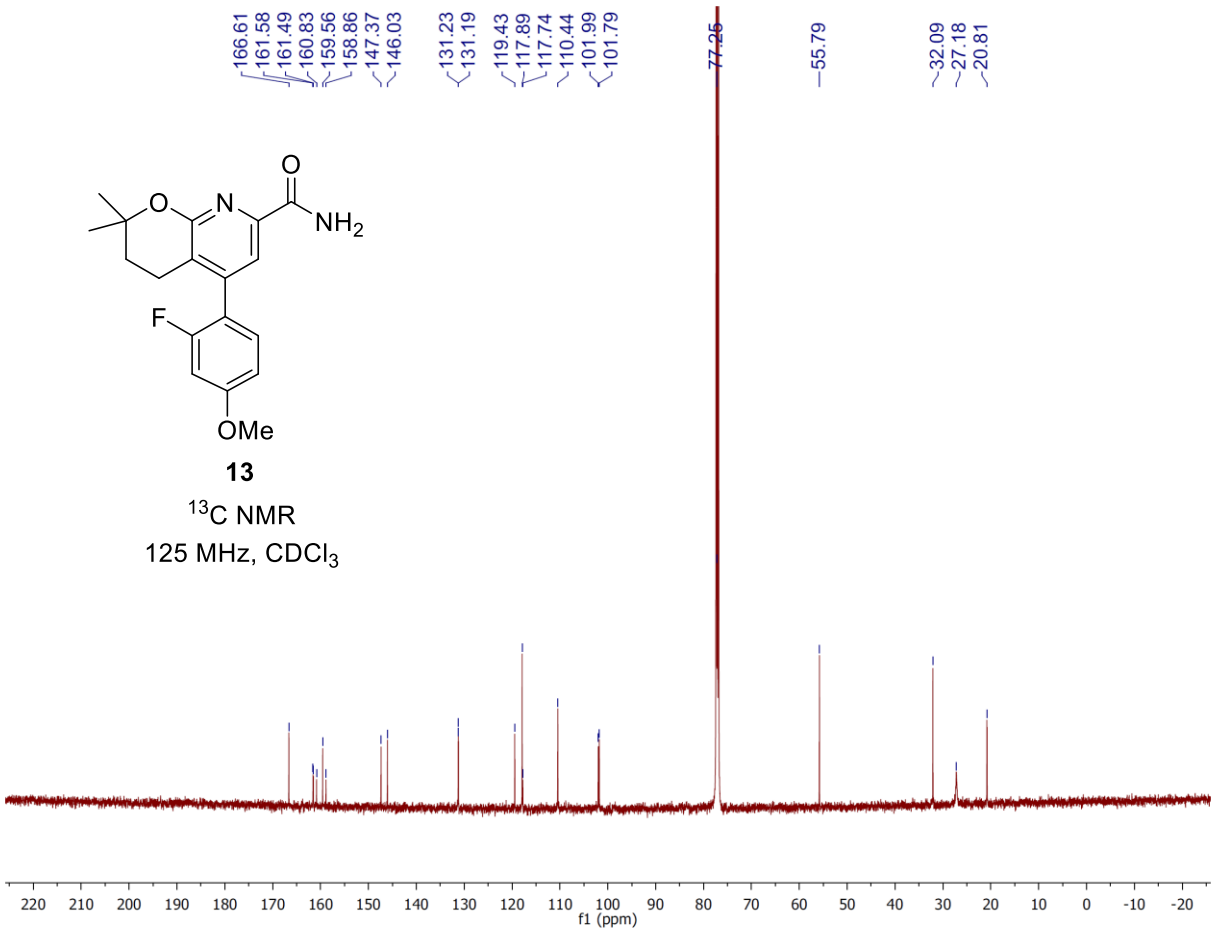

13

^{13}C NMR

125 MHz, $CDCl_3$

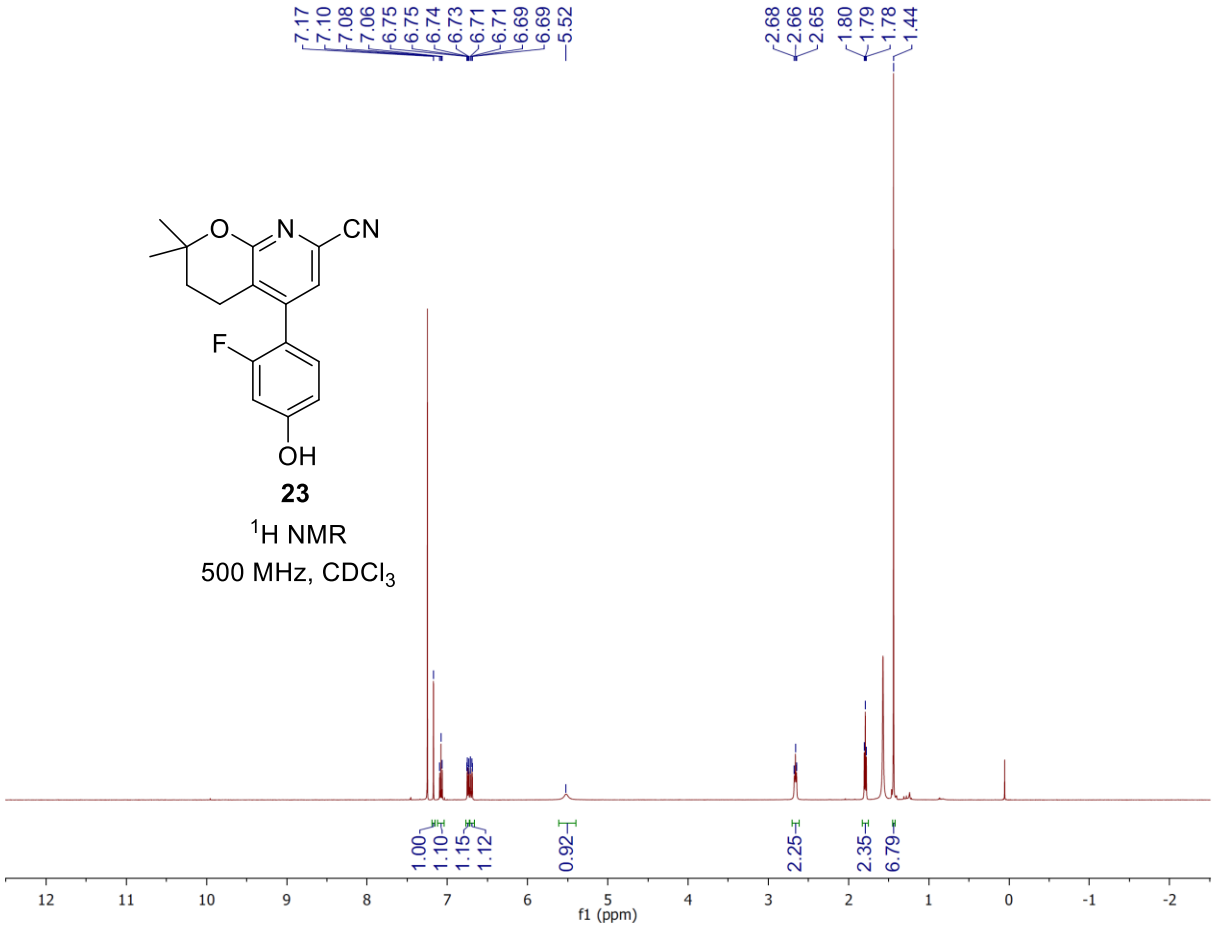
7.17
7.10
7.08
7.06
6.75
6.75
6.74
6.73
6.71
6.71
6.69
6.69
5.52
2.68
2.66
2.65
1.80
1.79
1.78
1.44
O
N
CN
F
OH
23
1H NMR
500 MHz, CDCl3
1.00
1.10
1.15
1.12
0.92
2.25
2.35
6.79
12
11
10
9
8
7
6
5
4
3
2
1
0
-1
-2
f1 (ppm)

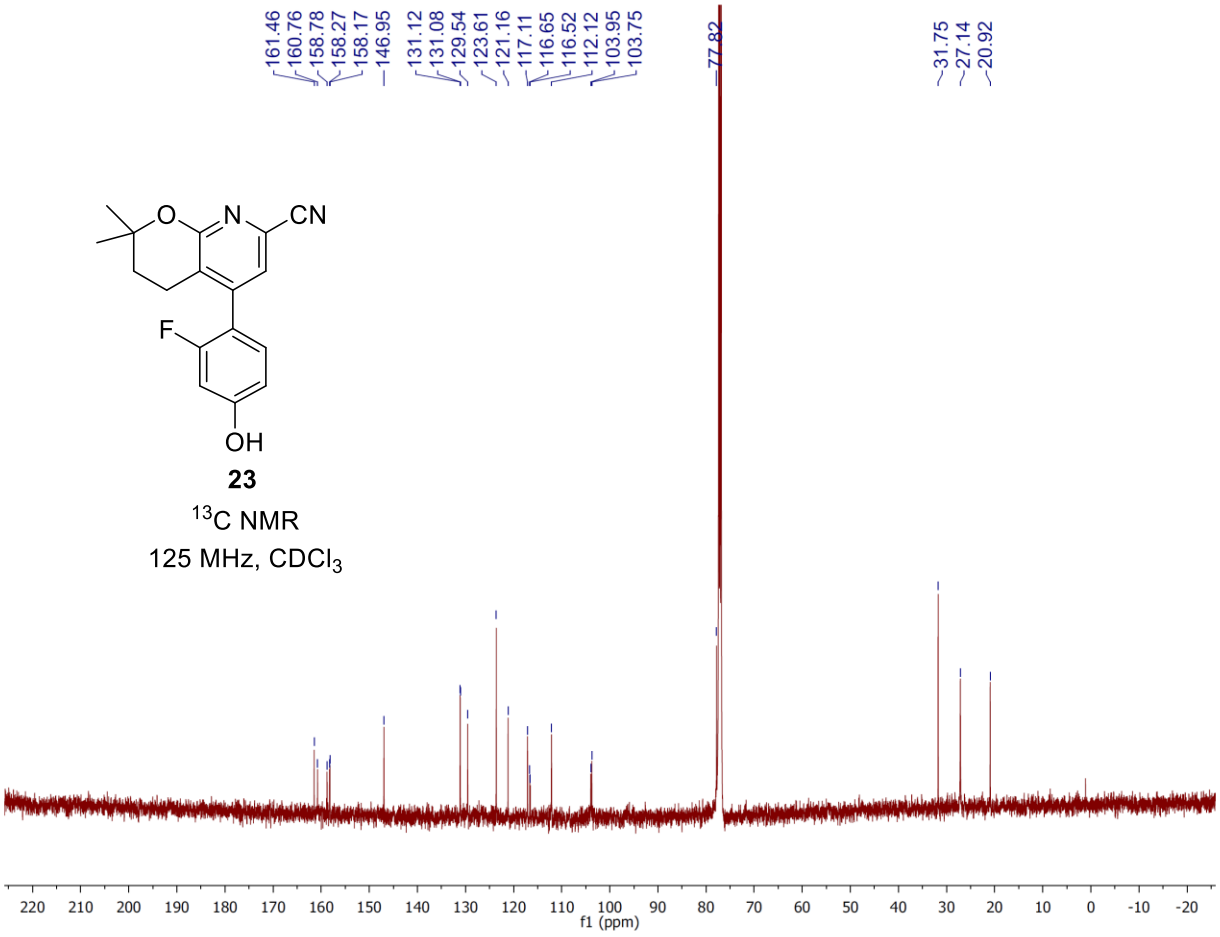
161.46
160.76
158.78
158.27
158.17
146.95
131.12
131.08
129.54
123.61
121.16
117.11
116.65
116.52
112.12
103.95
103.75
77.82
31.75
27.14
20.92
O
N
CN
F
OH
23
13C NMR
125 MHz, CDCl3
220 210 200 190 180 170 160 150 140 130 120 110 100 90 80 70 60 50 40 30 20 10 0 -10 -20
f1 (ppm)

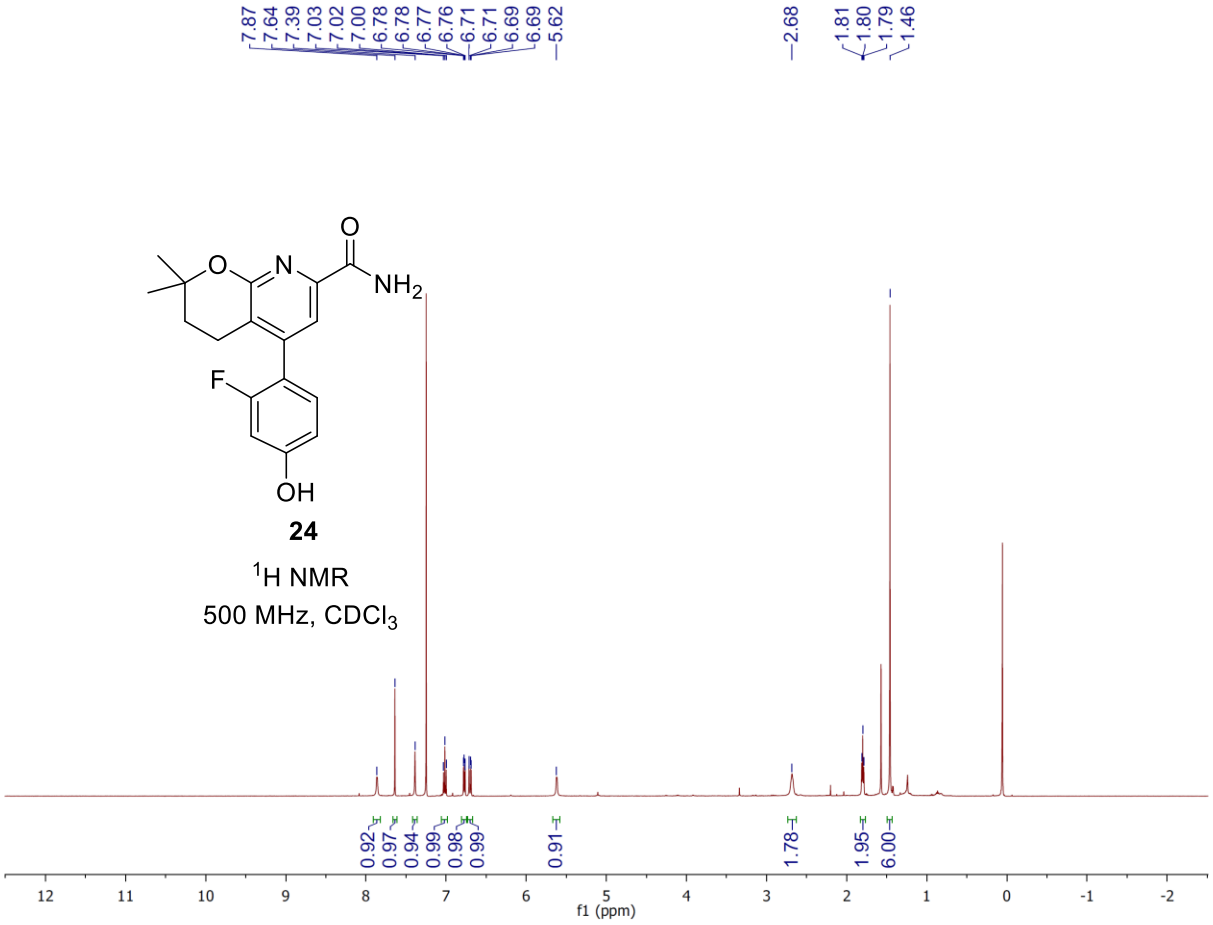
7.87
7.64
7.39
7.03
7.02
7.00
6.78
6.78
6.77
6.76
6.71
6.71
6.69
6.69
5.62
2.68
1.81
1.80
1.79
1.46
O
O
N
NH2
F
OH
24
1H NMR
500 MHz, CDCl3
0.92
0.97
0.94
0.99
0.98
0.99
0.91
1.78
1.95
6.00
12
11
10
9
8
7
6
5
4
3
2
1
0
-1
-2
f1 (ppm)

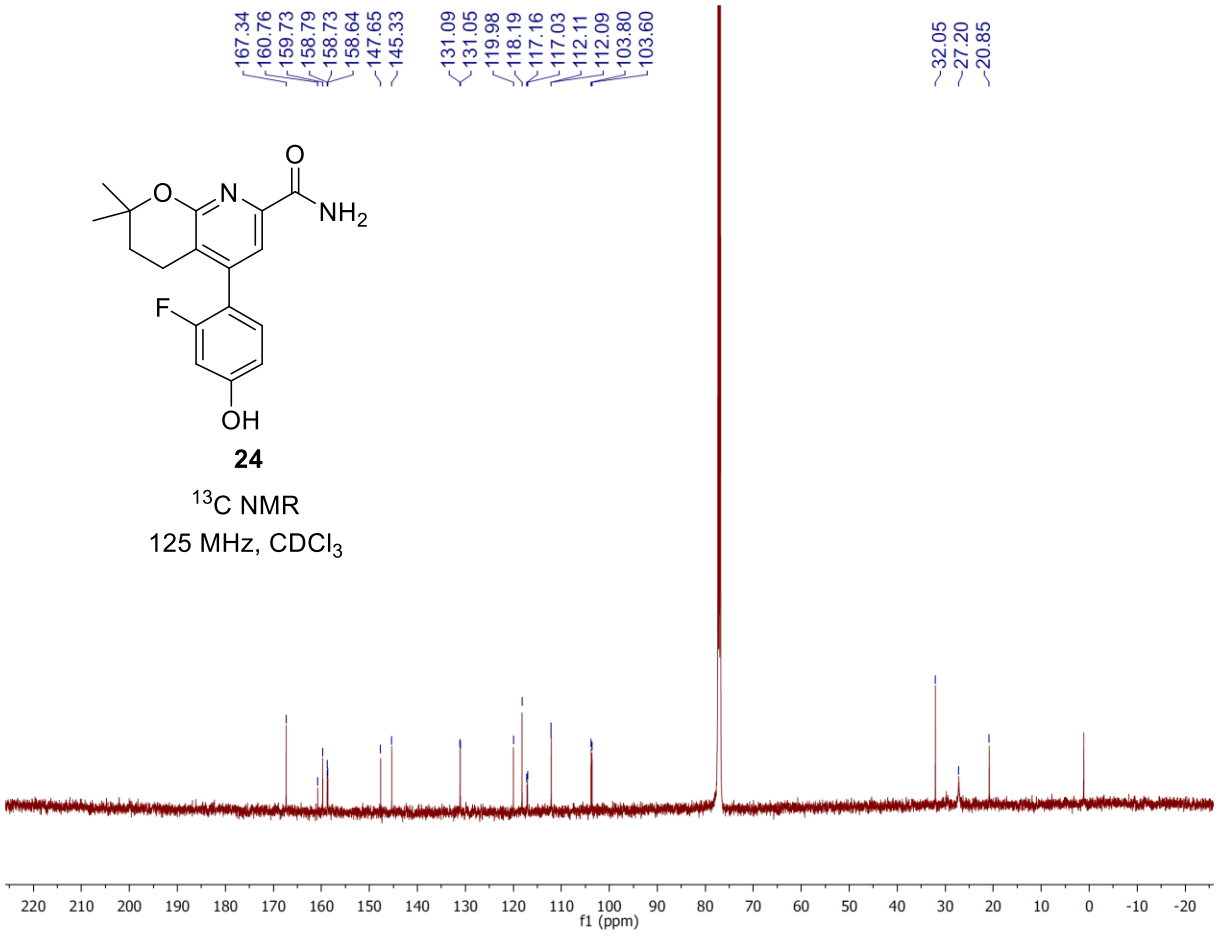

24

^{13}C NMR

125 MHz, $CDCl_3$

9. References

1. Krieger, E.; Joo, K.; Lee, J.; Lee, J.; Raman, S.; Thompson, J.; Tyka, M.; Baker, D.; Karplus, K. Improving physical realism, stereochemistry, and side-chain accuracy in homology modeling: Four approaches that performed well in CASP8. *Proteins.* **2009**, *77*, 114-122.
2. Dore, A. S.; Okrasa, K.; Patel, J. C.; Serrano-Vega, M.; Bennett, K.; Cooke, R. M.; Errey, J. C.; Jazayeri, A.; Khan, S.; Tehan, B.; Weir, M.; Wiggin, G. R.; Marshall, F. H. Structure of class C GPCR metabotropic glutamate receptor 5 transmembrane domain. *Nature.* **2014**, *511*, 557-562.
3. Wu, H.; Wang, C.; Gregory, K. J.; Han, G. W.; Cho, H. P.; Xia, Y.; Niswender, C. M.; Katritch, V.; Meiler, J.; Cherezov, V.; Conn, P. J.; Stevens, R. C. Structure of a class C GPCR metabotropic glutamate receptor 1 bound to an allosteric modulator. *Science.* **2014**, *344*, 58-64.
4. Koehl, A.; Hu, H.; Feng, D.; Sun, B.; Zhang, Y.; Robertson, M. J.; Chu, M.; Kobilka, T. S.; Laeremans, T.; Steyaert, J.; Tarrasch, J.; Dutta, S.; Fonseca, R.; Weis, W. I.; Mathiesen, J. M.; Skiniotis, G.; Kobilka, B. K. Structural insights into the activation of metabotropic glutamate receptors. *Nature.* **2019**, *566*, 79-84.
5. Chappell, M. D.; Li, R.; Smith, S. C.; Dressman, B. A.; Tromiczak, E. G.; Tripp, A. E.; Blanco, M. J.; Vetman, T.; Quimby, S. J.; Matt, J.; Britton, T. C.; Fivush, A. M.; Schkeryantz, J. M.; Mayhugh, D.; Erickson, J. A.; Bures, M. G.; Jaramillo, C.; Carpintero, M.; Diego, J. E.; Barberis, M.; Garcia-Cerrada, S.; Soriano, J. F.; Antonysamy, S.; Atwell, S.; MacEwan, I.; Condon, B.; Sougias, C.; Wang, J.; Zhang, A.; Conners, K.; Groshong, C.; Wasserman, S. R.; Koss, J. W.; Witkin, J. M.; Li, X.; Overshiner, C.; Wafford, K. A.; Seidel, W.; Wang, X. S.; Heinz, B. A.; Swanson, S.; Catlow, J. T.; Bedwell, D. W.; Monn, J. A.; Mitch, C. H.; Ornstein, P. L. Discovery of (1S,2R,3S,4S,5R,6R)-2-Amino-3-[(3,4-difluorophenyl)sulfanylmethyl]-4-hydroxy-bicyclo[3.1.0]hexane-2,6-dicarboxylic Acid Hydrochloride (LY3020371.HCl): A Potent, Metabotropic Glutamate 2/3 Receptor Antagonist with Antidepressant-Like Activity. *J. Med. Chem.* **2016,** *59*, 10974-10993.
6. Altschul, S. F.; Madden, T. L.; Schaffer, A. A.; Zhang, J. H.; Zhang, Z.; Miller, W.; Lipman, D. J. Gapped BLAST and PSI-BLAST: a new generation of protein database search programs. *Nucleic Acids Res.* **1997**, *25*, 3389-3402.
7. McGuffin, L. J.; Shuid, A. N.; Kempster, R.; Maghrabi, A. H. A.; Nealon, J. O.; Salehe, B. R.; Atkins, J. D.; Roche, D. B. Accurate template-based modeling in CASP12 using the IntFOLD4-TS, ModFOLD6, and ReFOLD methods. *Proteins.* **2018,** *86*, 335-344.
8. Eisenberg, D.; Luthy, R.; Bowie, J. U. VERIFY3D: assessment of protein models with three-dimensional profiles. *Methods Enzymol.* **1997**, *277*, 396-404.
9. Waterhouse, A.; Bertoni, M.; Bienert, S.; Studer, G.; Tauriello, G.; Gumienny, R.; Heer, F. T.; de Beer, T. A. P.; Rempfer, C.; Bordoli, L.; Lepore, R.; Schwede, T. SWISS-MODEL: homology modelling of protein structures and complexes. *Nucleic Acids Res.* **2018**, *46*, W296-W303.
10. Colovos, C.; Yeates, T. O. Verification of protein structures: patterns of nonbonded atomic interactions. *Protein Sci.* **1993**, *2*, 1511-1519.
11. Tong, W. X.; Wei, Y.; Murga, L. F.; Ondrechen, M. J.; Williams, R. J. Partial Order Optimum Likelihood (POOL): Maximum Likelihood Prediction of Protein Active Site Residues Using 3D Structure and Sequence Properties. *PLoS Comput. Biol.* **2009,** *5*, e1000266.
12. Somarowthu, S.; Yang, H.; Hildebrand D. G. C.; Ondrechen, M. J. High performance prediction of functional residues in proteins with machine learning and computed input features. *Biopolymers.* **2011**, *95*, 390-400.

13. Ringe, D.; Wei, Y.; Boino, K. R.; Ondrechen, M. J. Protein structure to function: insights from computation. *Cell Mol. Life Sci.* **2004**, *61*, 387-392.
14. Shehadi, I. A.; Abyzov, A.; Uzun, A.; Wei, Y.; Murga, L. F.; Ilyin, V.; Ondrechen, M. J. Active site prediction for comparative model structures with thematics. *J. Bioinform. Comput. Biol.* **2005**, *3*, 127-143.
15. Harpsoe, K.; Isberg, V.; Tehan, B. G.; Weiss, D.; Arsova, A.; Marshall, F. H.; Brauner-Osborne, H.; Gloriam, D. E. Selective Negative Allosteric Modulation Of Metabotropic Glutamate Receptors - A Structural Perspective of Ligands and Mutants. *Sci. Rep.* **2015**, *5*, 13869.
16. Hemstapat, K.; Da Costa, H.; Nong, Y.; Brady, A. E.; Luo, Q.; Niswender, C. M.; Tamagnan, G. D.; Conn, P. J. A novel family of potent negative allosteric modulators of group II metabotropic glutamate receptors. *J. Pharmacol. Exp. Ther.* **2007**, *322*, 254-264.
17. Rydberg, P.; Gloriam, D. E.; Zaretzki, J.; Breneman, C.; Olsen, L. SMARTCyp: A 2D Method for Prediction of Cytochrome P450-Mediated Drug Metabolism. *ACS Med. Chem. Lett.* **2010**, *1*, 96-100.